

---

***Project 31-L: Accumulative Roll Bonding of Al Sheets  
(AA 5083) Toward Low Temperature Superplasticity***

***Semi-annual Spring Meeting  
April 2022***

- Student: Brady McBride (Mines, now ATI Specialty Materials)
- Advisors: Kester Clarke (Mines), Amy Clarke (Mines)
- Industrial Mentors: John Carpenter (LANL), Eric Payton (AFRL)

# Project 31-L: Accumulative Roll Bonding of Al Sheets Toward Low Temperature Superplasticity



- Student: Brady McBride (Mines)
- Advisor(s): Kester Clarke (Mines)

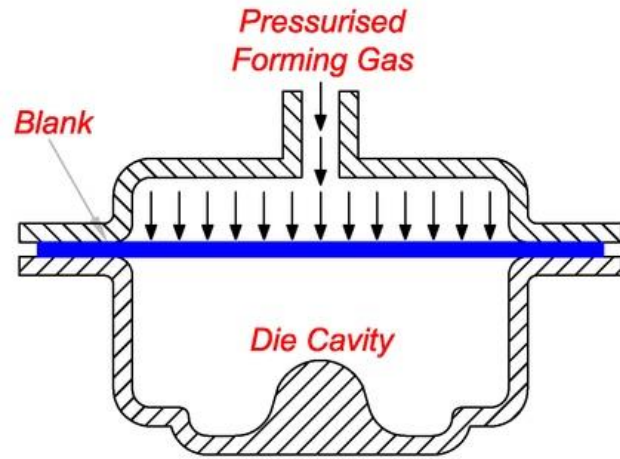
**Project Duration**  
PhD: September 2017 to December 2021

- **Problem:** Superplastic forming requires high temperatures and very low strain rates.
- **Objective:** Develop an in-depth understanding of how accumulative roll bonding affects temperature dependent strength and superplastic properties of Al alloys.
- **Benefit:** Low temperature superplasticity could result in reduced cost and cycle time due to reduced deformation temperatures and increased strain rates.

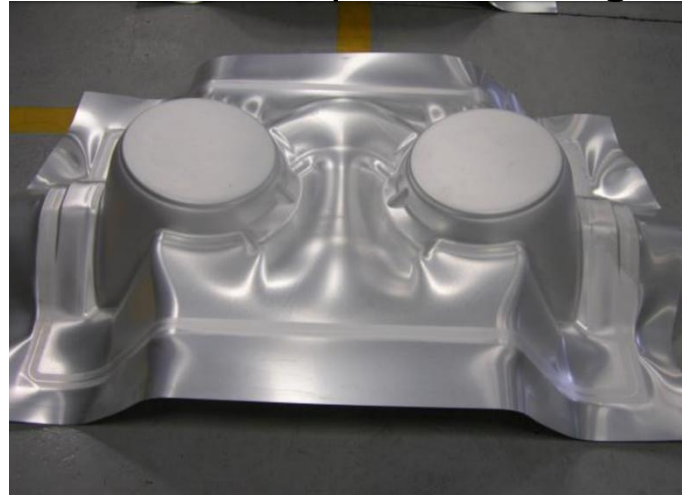
- Recent Progress** (Defended PhD thesis, December 2021)
- **“Continuous recrystallization during annealing** of AA 5083 produced by accumulative roll bonding (ARB)”, *Metall. & Mater. Trans. A*, submitted February 2022.
  - **“The limits of low temperature superplasticity** in AA 5083 produced by accumulative roll bonding (ARB)”, *Metall. & Mater. Trans. A*, submitted March 2022.
  - **“Biaxial low temperature superplasticity** in AA 5083 produced by accumulative roll bonding (ARB)”, *J. Mater. Perform. Eng.*, submitted April 2022.

Metrics		
Description	% Complete	Status
1. Develop ARB process with mitigated edge cracking	100%	●
2. Identify optimal conditions for low temperature superplasticity through tensile testing	100%	●
3. Characterize microstructure evolution with ARB processing and tensile deformation	100%	●
4. Formalize limits for low temperature superplasticity based on kinetics of deformation	100%	●
5. Characterize small-scale formability testing specimens	100%	●

# Industrial Relevance: Superplastic Forming



Aircraft lamp can housing

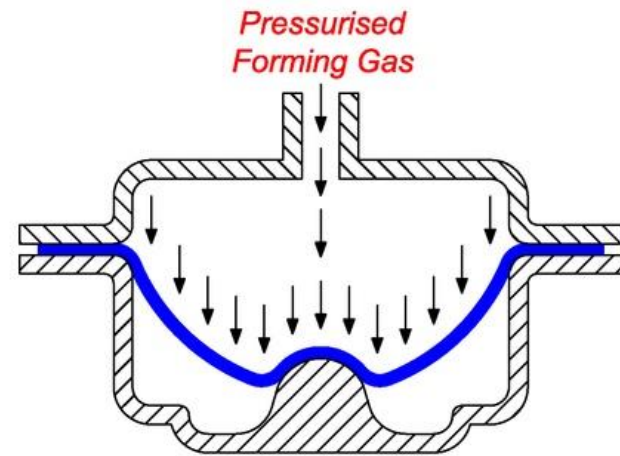


Barnes et al., *Mat. Sci. Forum*, 2003.

2018 Bentley Continental GT



LightMetalAge



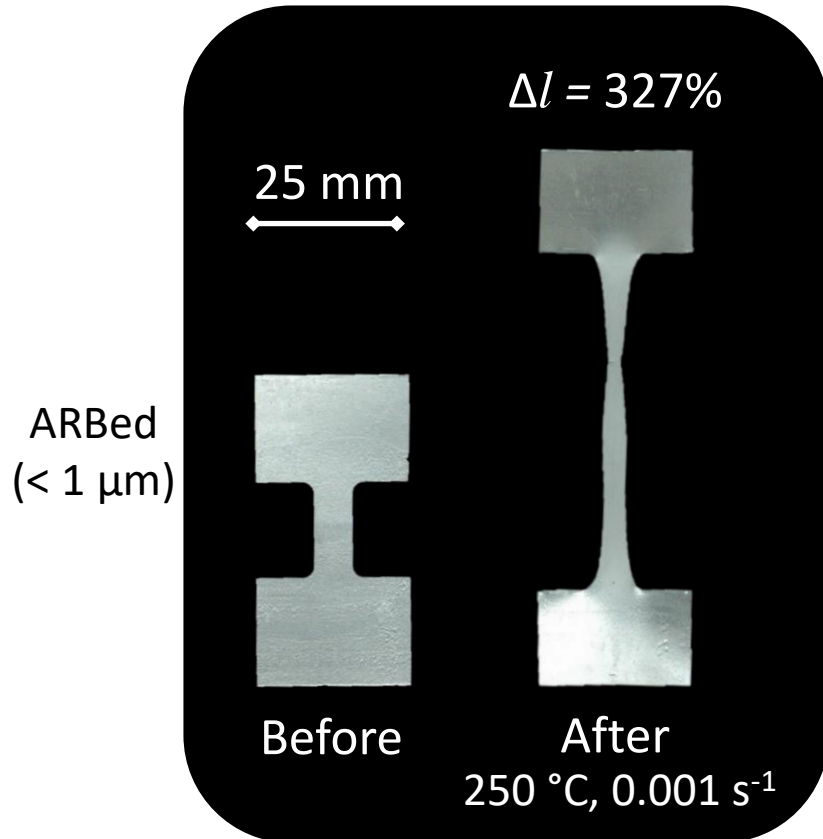
LightMetalAge

Conventionally processed AA 5083:

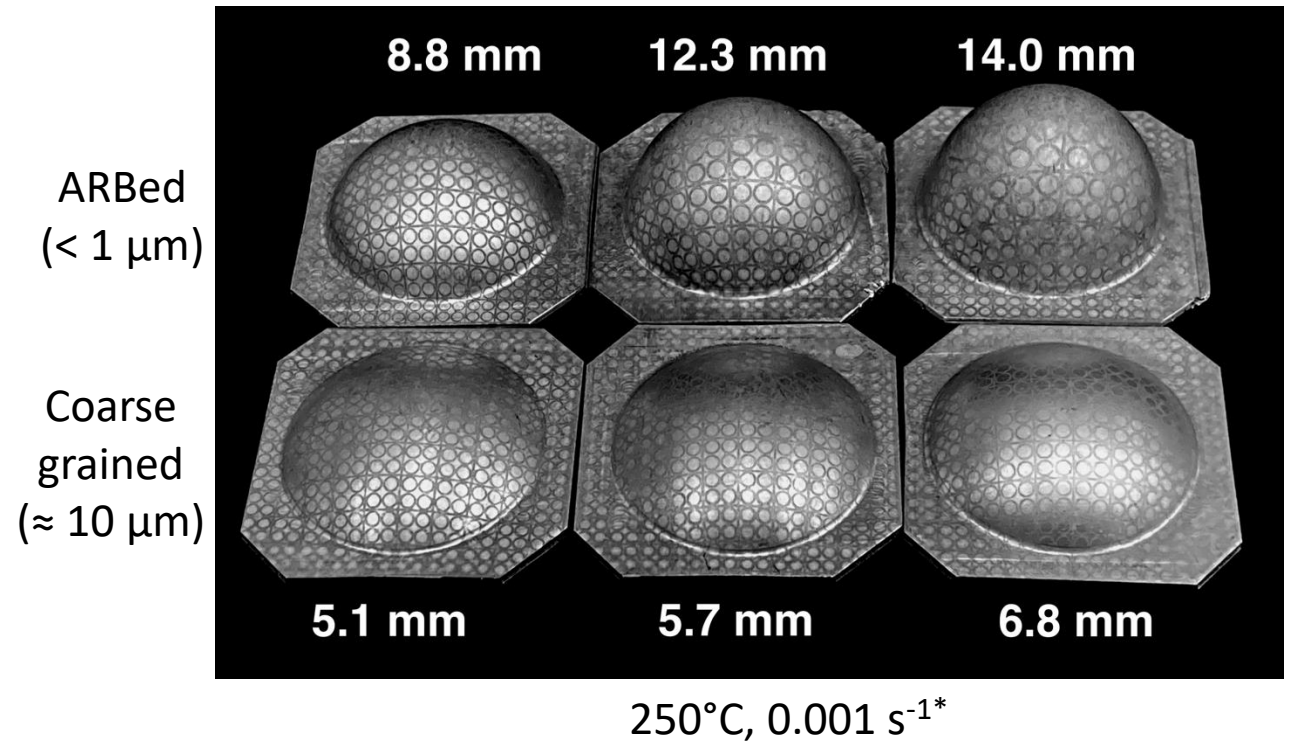
Grain size:	10 $\mu\text{m}$
Temperature:	500°C
Strain rates:	1 x 10 <sup>-3</sup> s <sup>-1</sup>
Thinning ratios:	2.0
Void fraction:	2%

# Industrial Relevance: Reduced Temperature Formability

Uniaxial tension



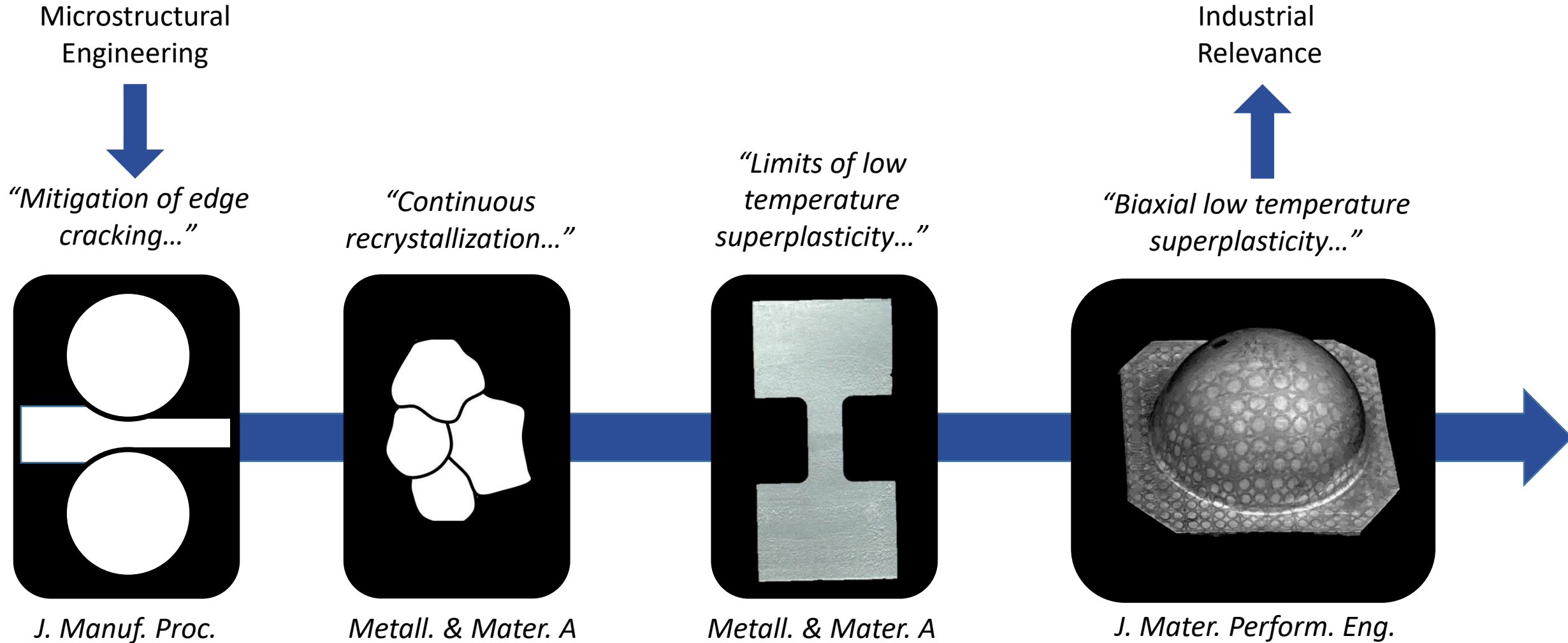
Biaxial bulge testing



\*load-controlled nominal strain rate

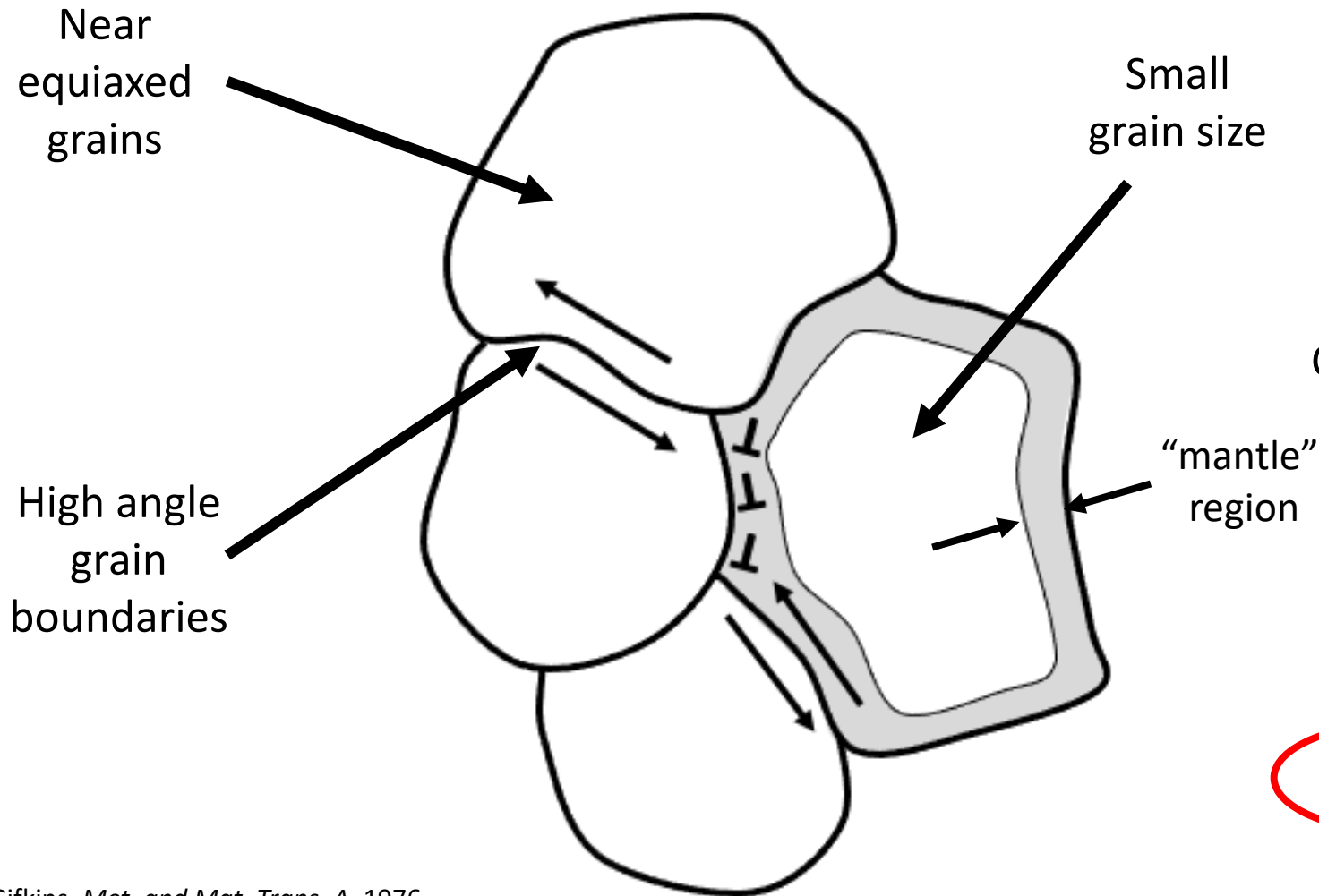


# Project Overview & Milestones



# Introduction: Superplasticity

Gifkins grain boundary diffusion accommodation model



Conventional superplasticity in AA 5083:

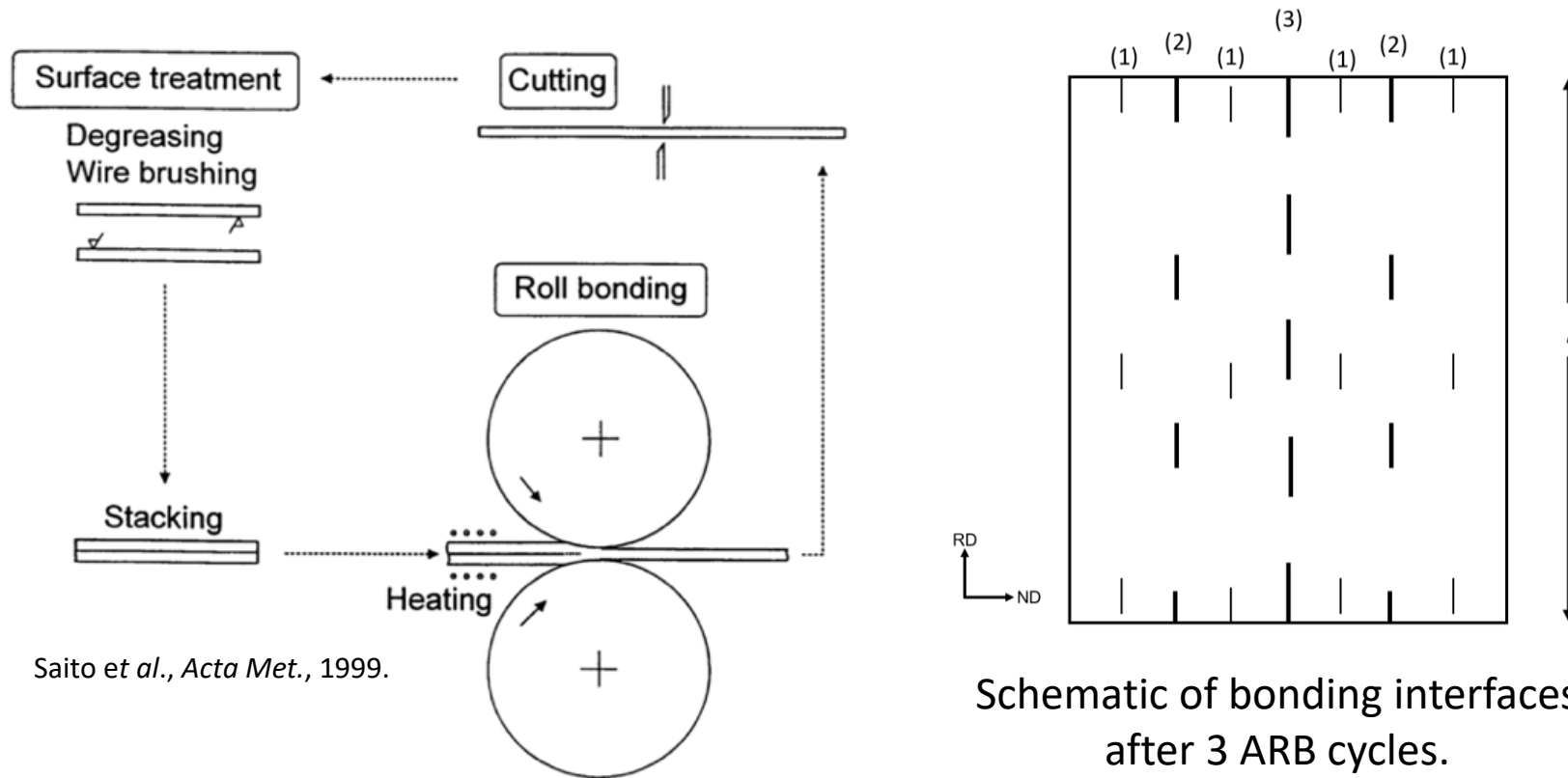
$$\dot{\epsilon} = A \frac{DGb}{kT} \left(\frac{b}{d}\right)^p \left(\frac{\sigma}{G}\right)^{\frac{1}{m}}$$

$T > 500^\circ\text{C}$

$10 \mu\text{m}$

Gifkins, *Met. and Mat. Trans. A*, 1976.

# Accumulative Roll Bonding (ARB)



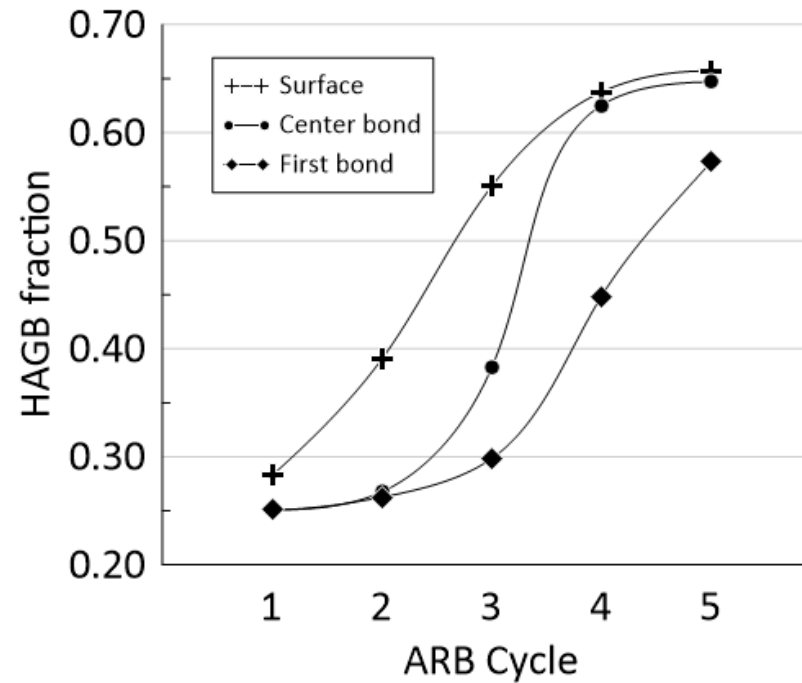
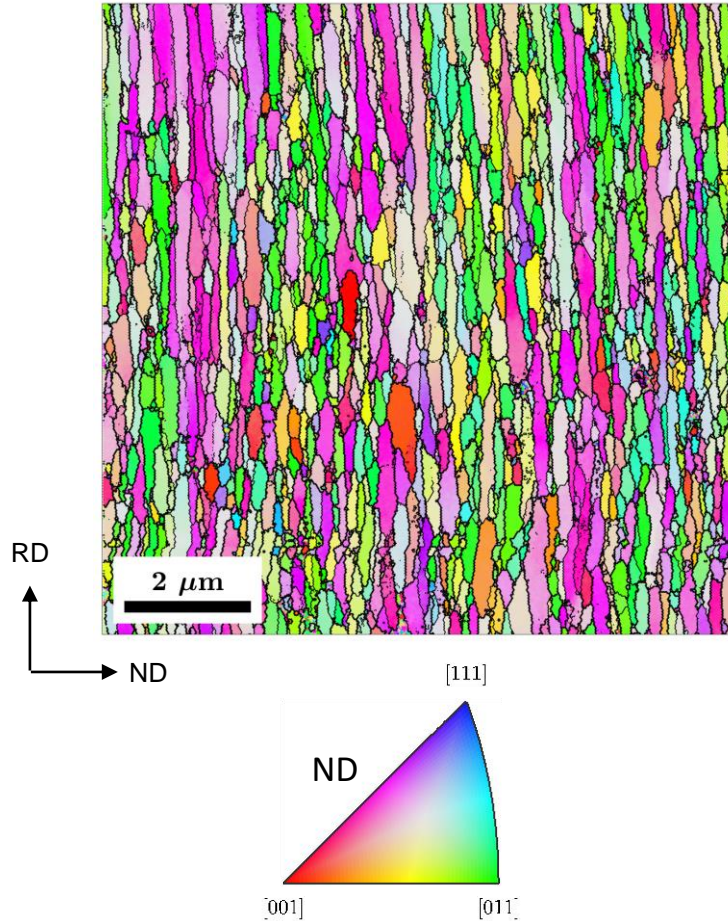
Saito et al., *Acta Met.*, 1999.

Schematic of bonding interfaces after 3 ARB cycles.

- Outcomes of ARB:
- laminate sheet
  - interface development
  - strain retention

# Grain Refinement through ARB

Mid-thickness grain morphology  
after 5 ARB cycles

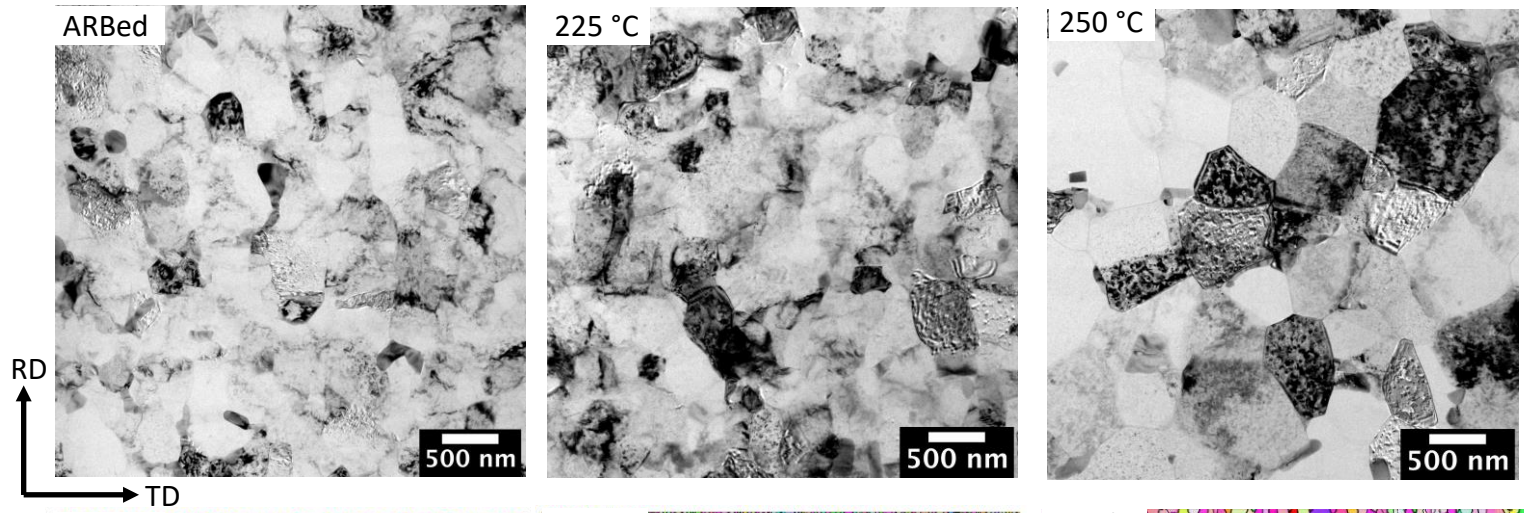


*in-situ* recrystallization:  
- submicron grain size  
- large HAGB fraction



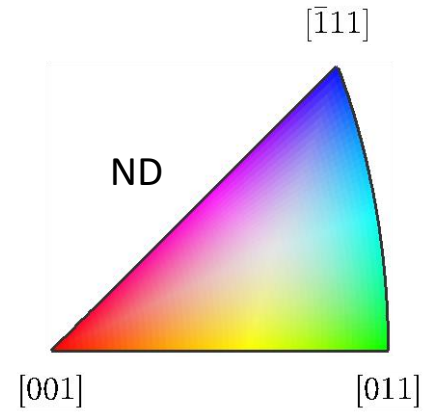
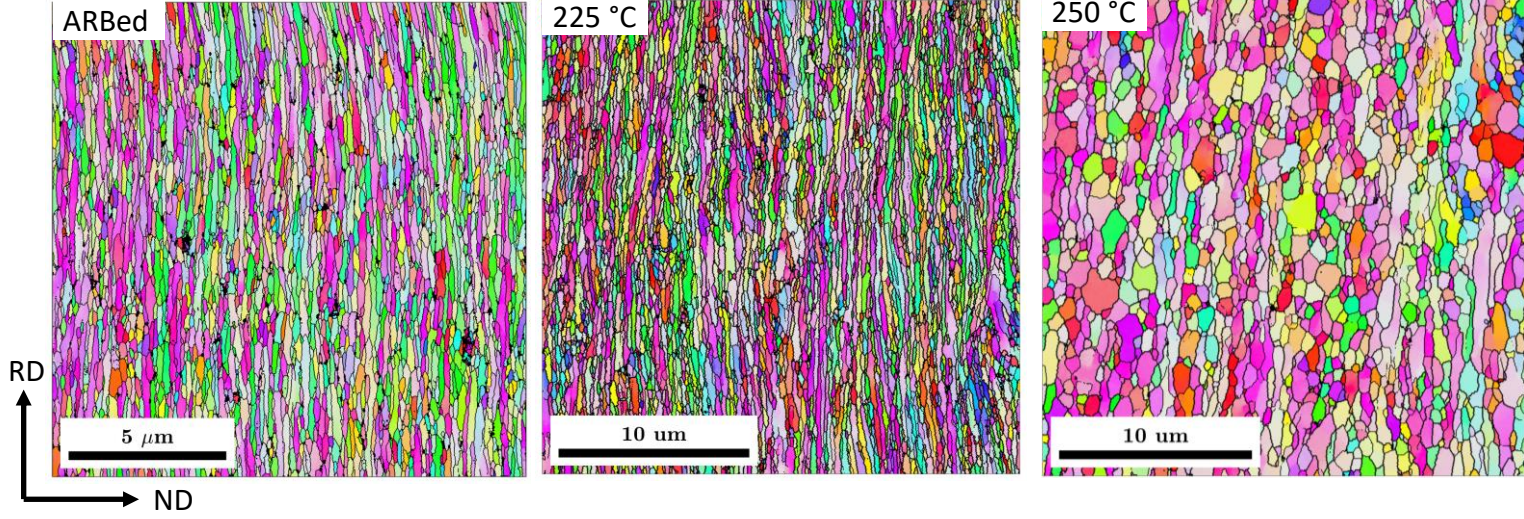
# Evidence for Continuous Recrystallization

15 minute static anneal treatments



Continuous recrystallization  
between 225 and 250°C  
due to large HAGB fraction

Significant grain growth  
above 250°C



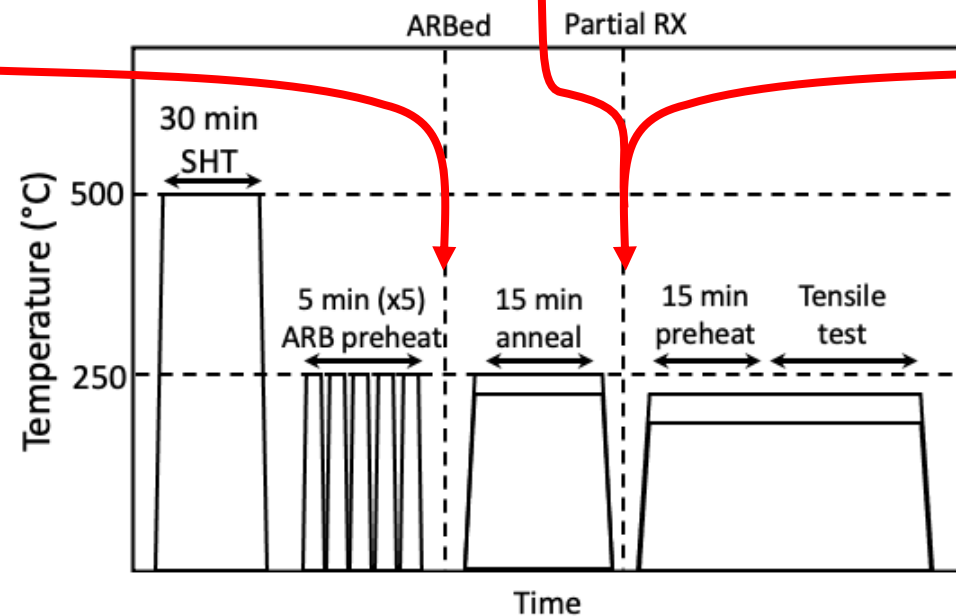
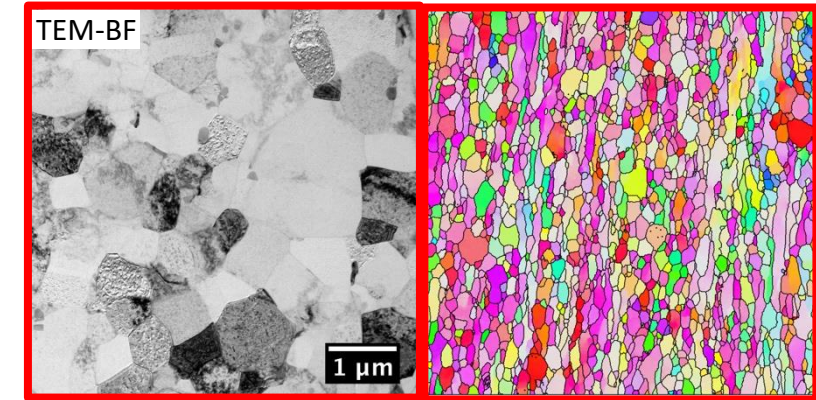
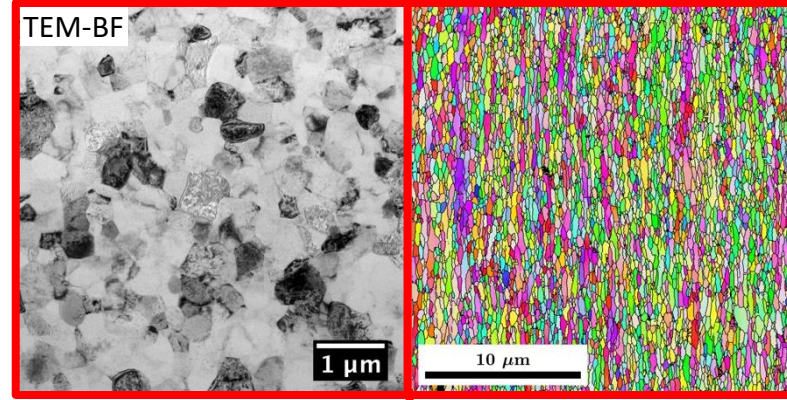
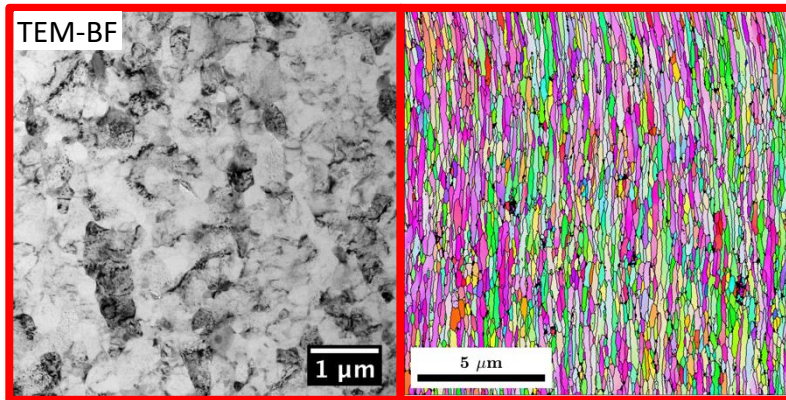


# Effect of Partial Recrystallization on Tensile Response

ARBed condition

240°C, 15min

250°C, 15min

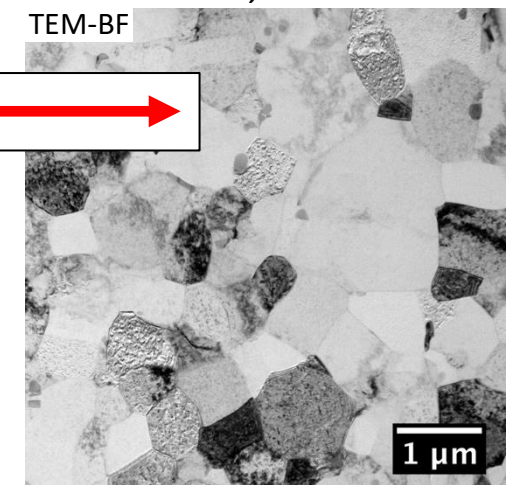
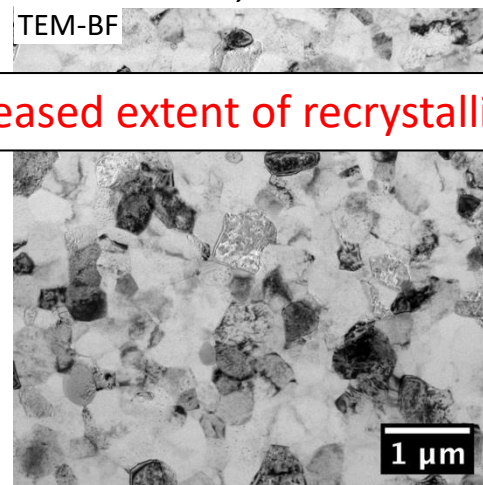
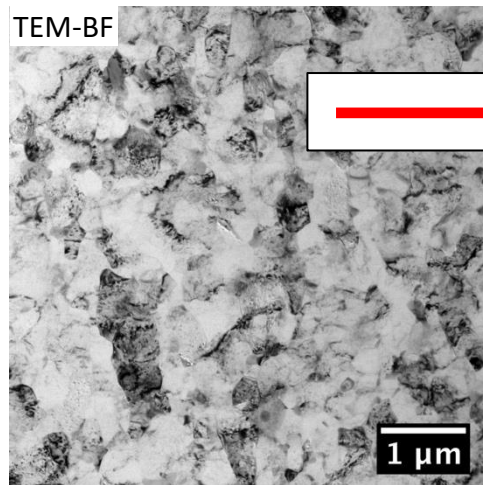


# Effects of Partial Recrystallization on Tensile Response

ARBed condition

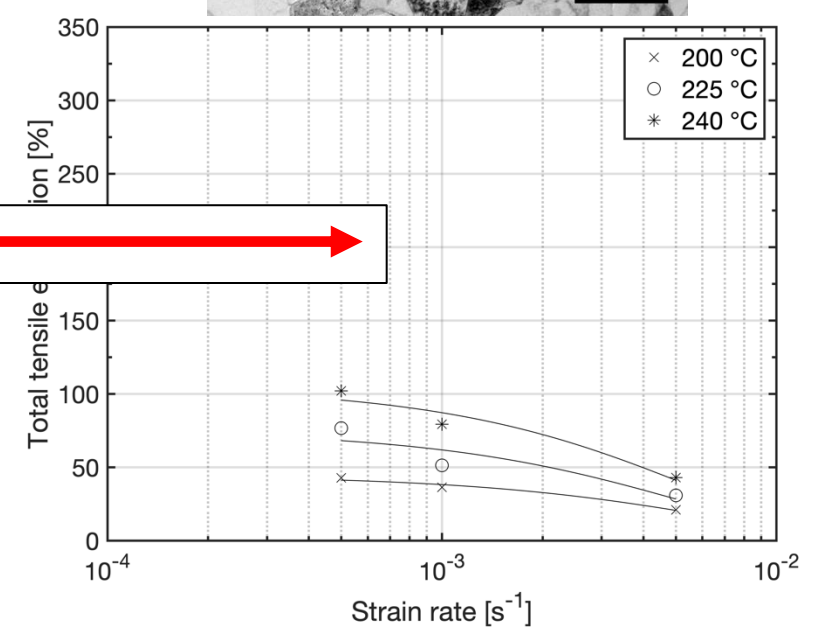
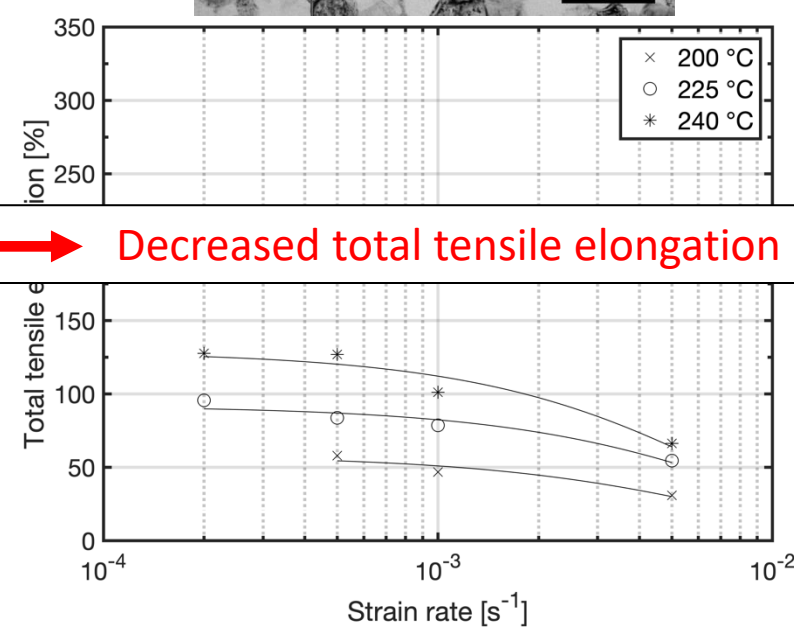
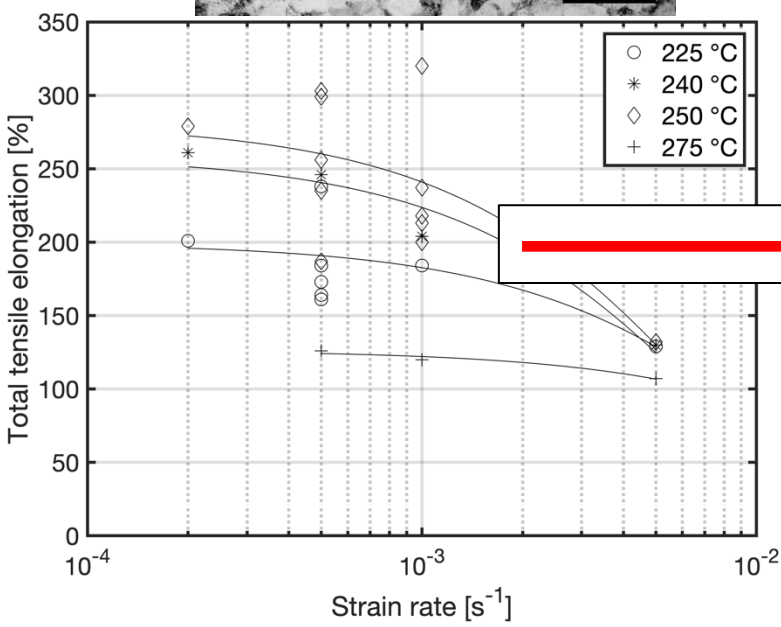
240°C, 15min

250°C, 15min



Increased extent of recrystallization

Decreased total tensile elongation



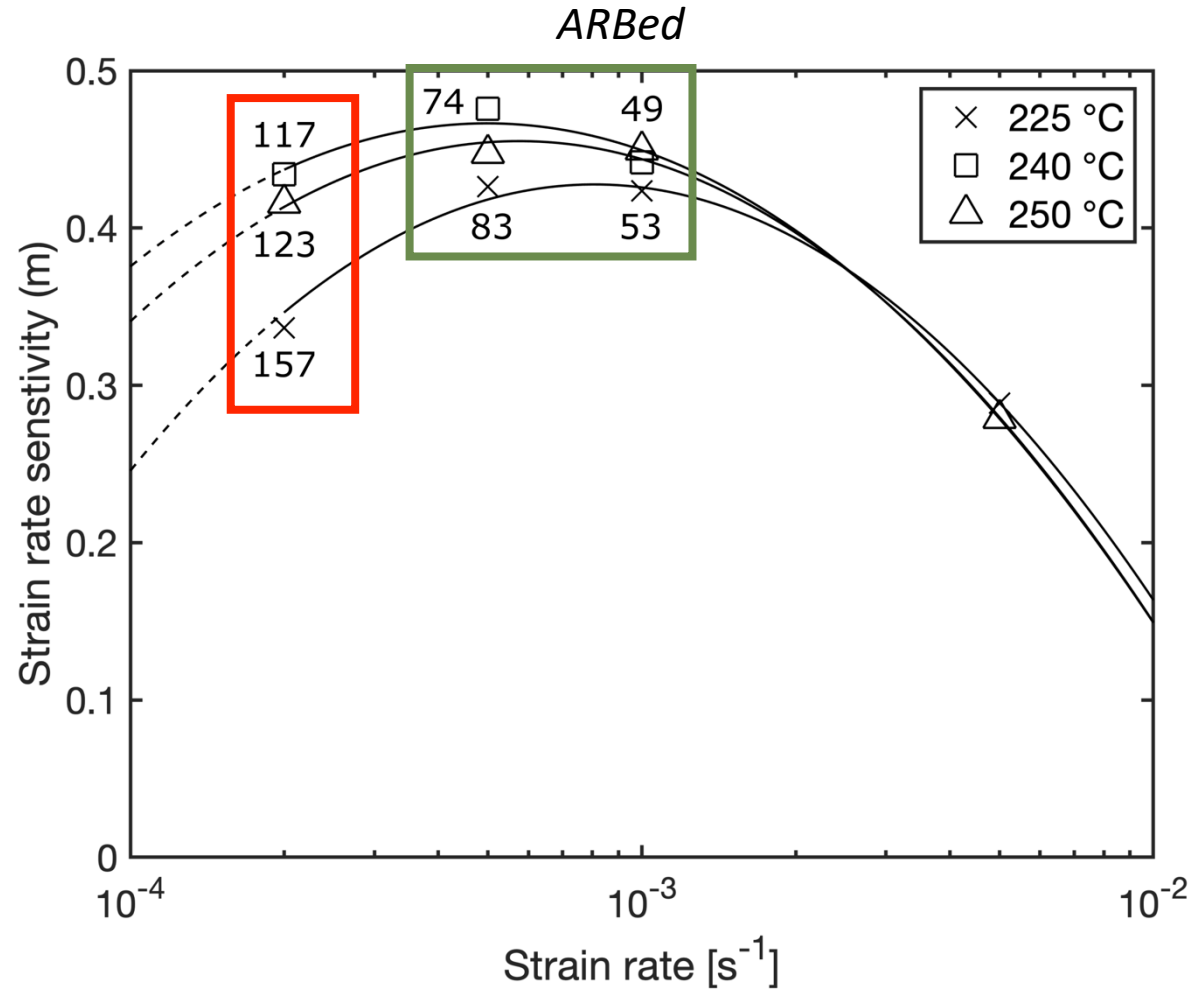
# Conclusions: Microstructural Stability



1. ARBed microstructure is **submicron** with **large HAGB fraction**.
2. Microstructure is **resistant to discontinuous recrystallization** due to large HAGB fraction.
3. Total tensile elongation **decreases with** extent of **static annealing**.



# Identifying Deformation Mechanisms

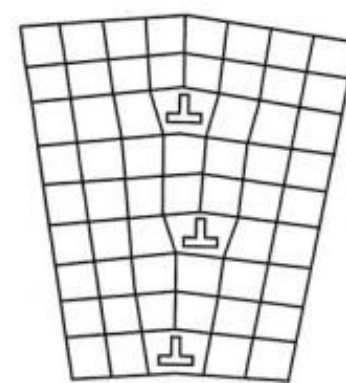
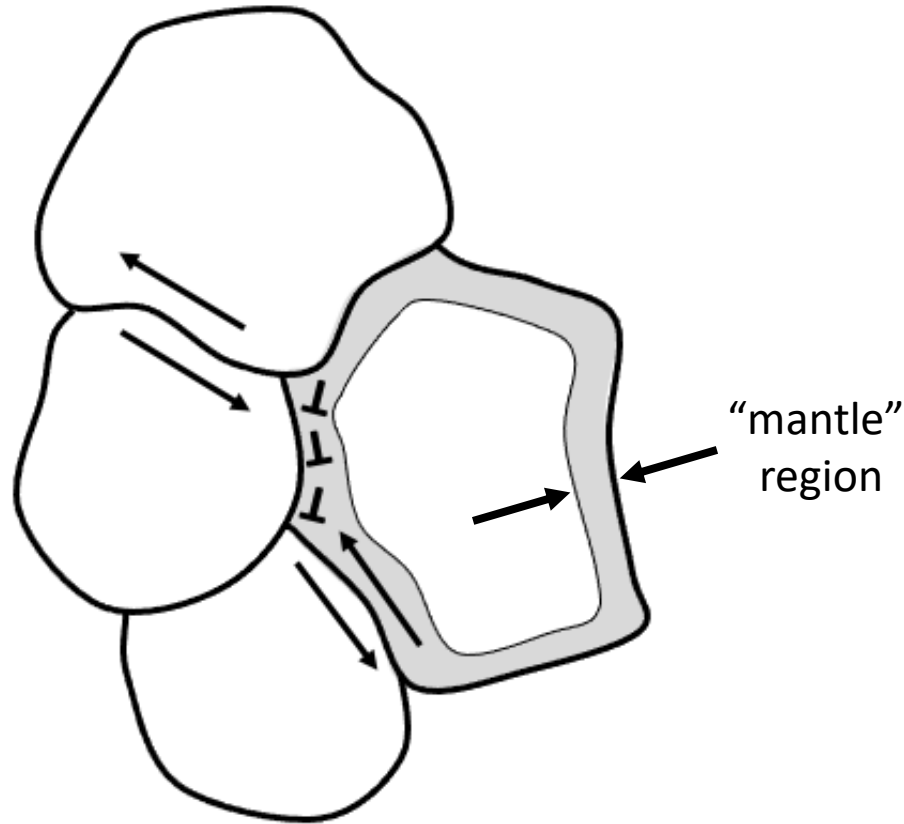


Gifkin's model for grain boundary sliding:

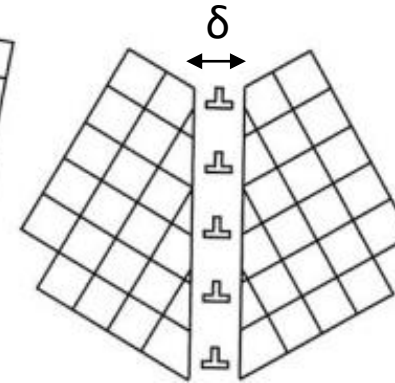
$$\dot{\epsilon} = A \frac{D_0 G b}{kT} \left(\frac{b}{d}\right)^p \left(\frac{\sigma}{G}\right)^{\frac{1}{m}} e^{\frac{-Q}{kT}}$$

Q<sub>GB</sub> ≈ 84 kJ/mol  
m<sub>GB</sub> ≈ 0.5

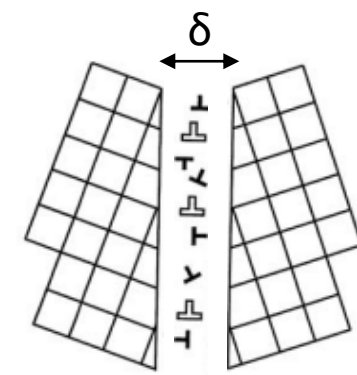
# The Significance of Grain Boundary Character



Low angle  
grain boundary



High angle  
grain boundary

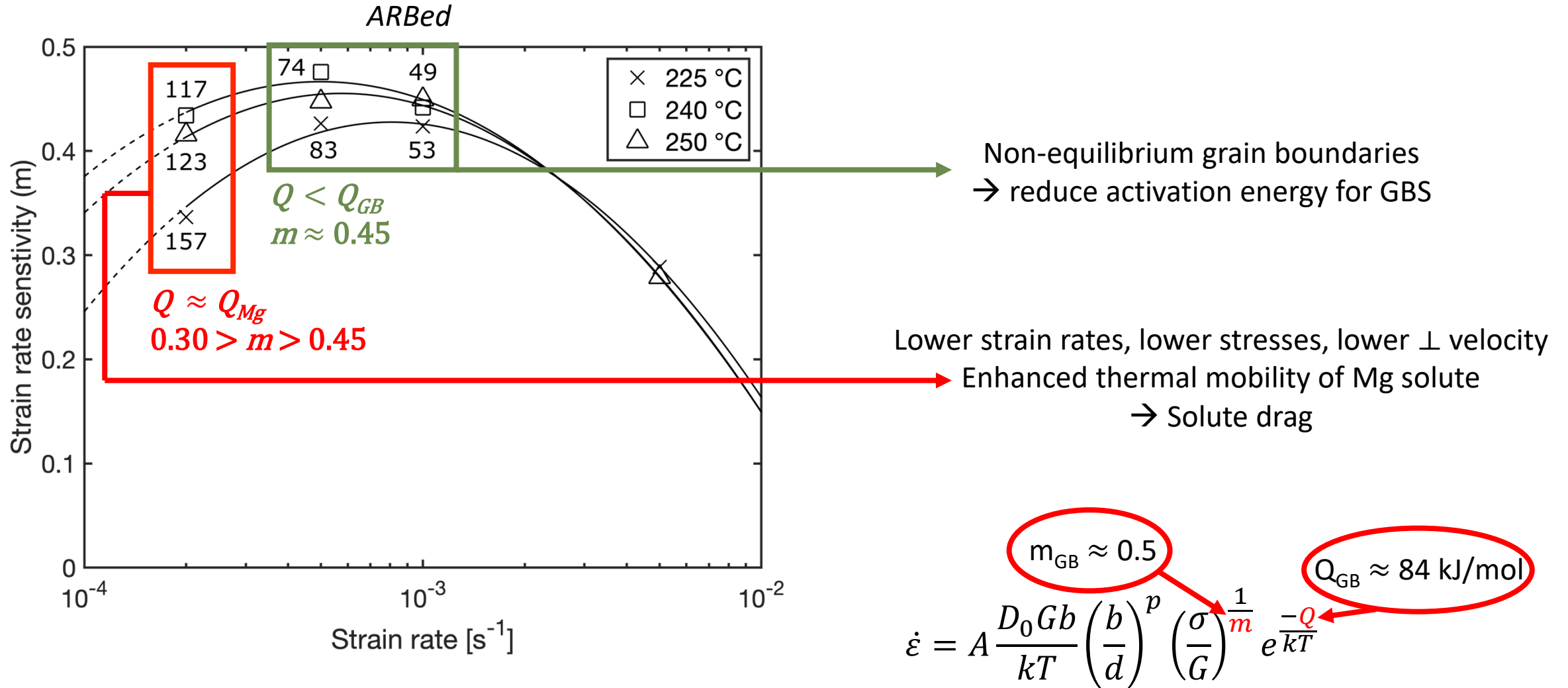


Non-equilibrium  
high angle  
grain boundary

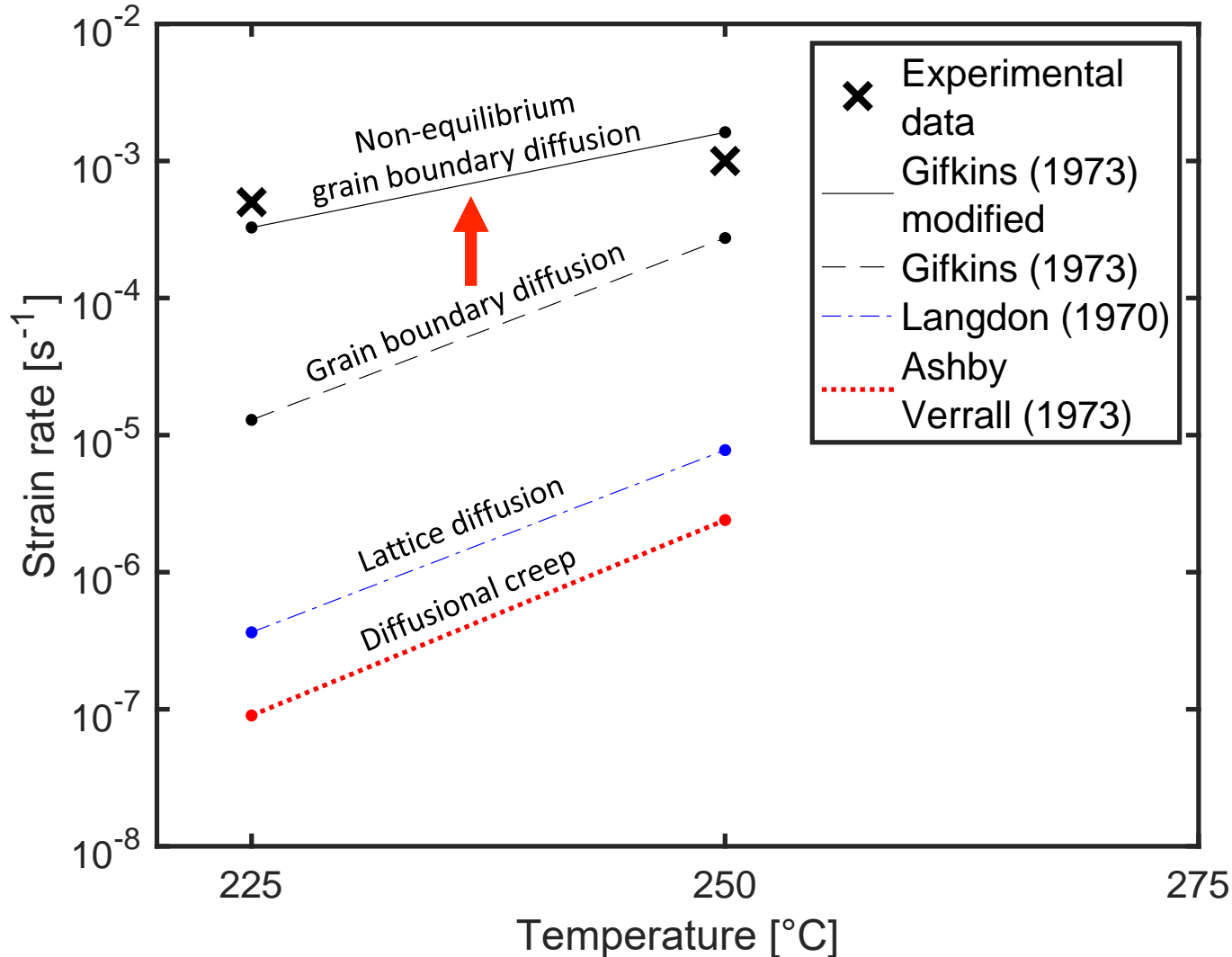
Non-equilibrium grain boundaries have:

- larger widths,  $\delta$
- **higher diffusivities (lower activation energy)**
- possible solute segregation (Mg)

# Identifying Primary Deformation Mechanisms



# Comparison to Grain Boundary Sliding Models



$$\dot{\epsilon} = A \frac{D_0 G b}{kT} \left(\frac{b}{d}\right)^p \left(\frac{\sigma}{G}\right)^{\frac{1}{m}} e^{\frac{-Q}{kT}}$$

Grain boundary sliding models predict significantly lower strain rates

Modifications to Gifkins core-mantle model:

1. Grain boundary width  $\approx 4\delta$
2. Activation energy  $\approx 0.5 Q_{GB}$

results in 10<sup>2</sup> – 10<sup>3</sup> increase in diffusivity [m<sup>2</sup>/s]

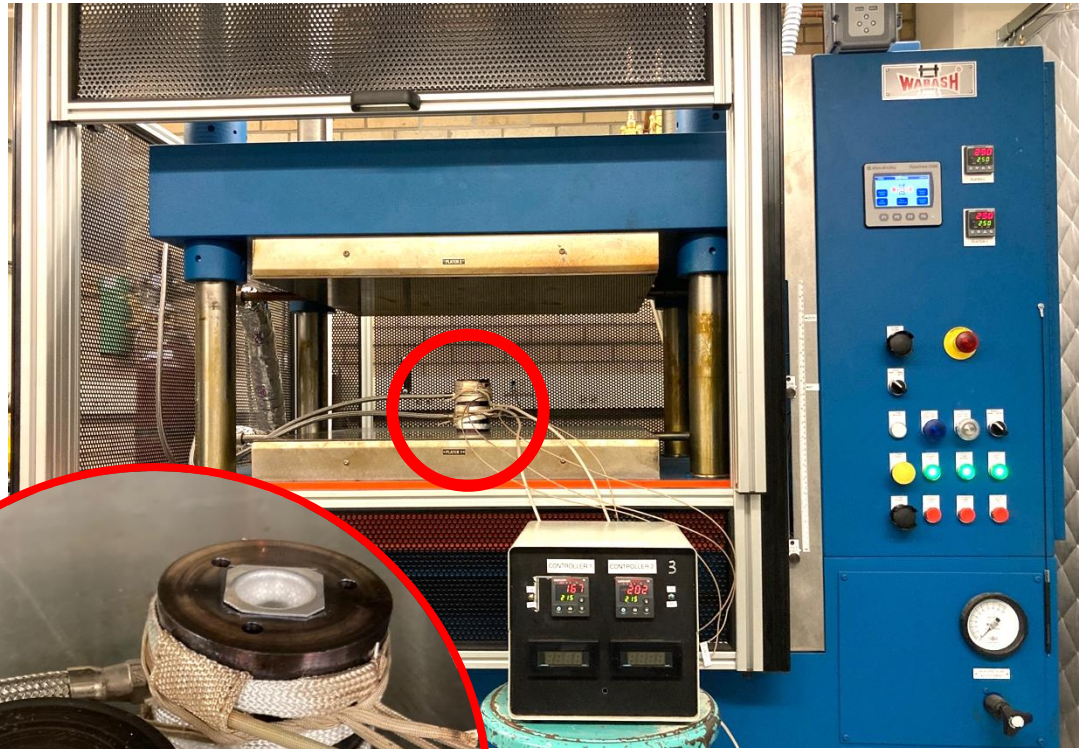


# Conclusions: Uniaxial Tensile Performance

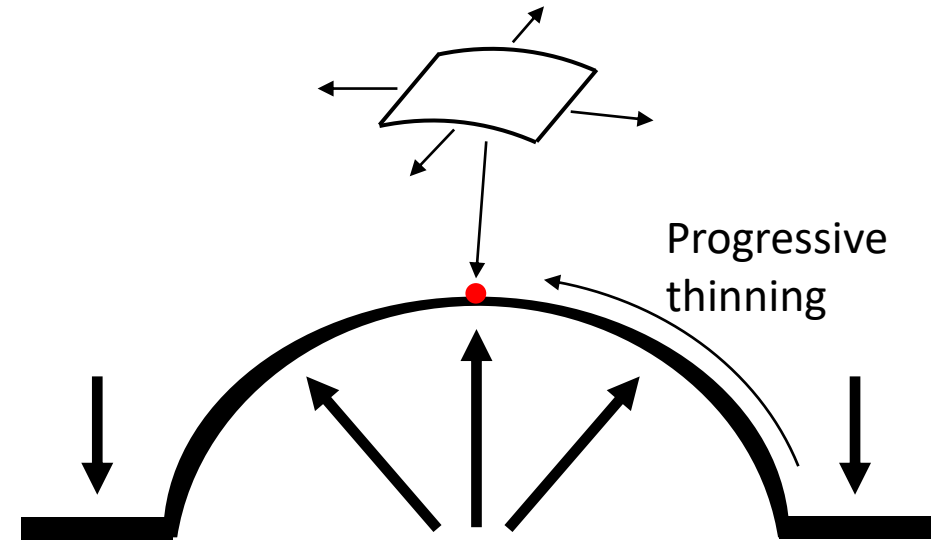


1. Grain boundary sliding occurs with lower activation energies than conventionally reported (84 kJ/mol).
2. **Non-equilibrium HAGBs** likely responsible for increasing grain boundary diffusion rates.
3. **Partial static recrystallization** leads equilibrium grain boundary structure.
4. Solute partitioning (Mg) to grain boundaries may contribute to **enhanced solute drag** at low temperatures and strain rates.

# Biaxial Bulge Testing



Biaxial stress state

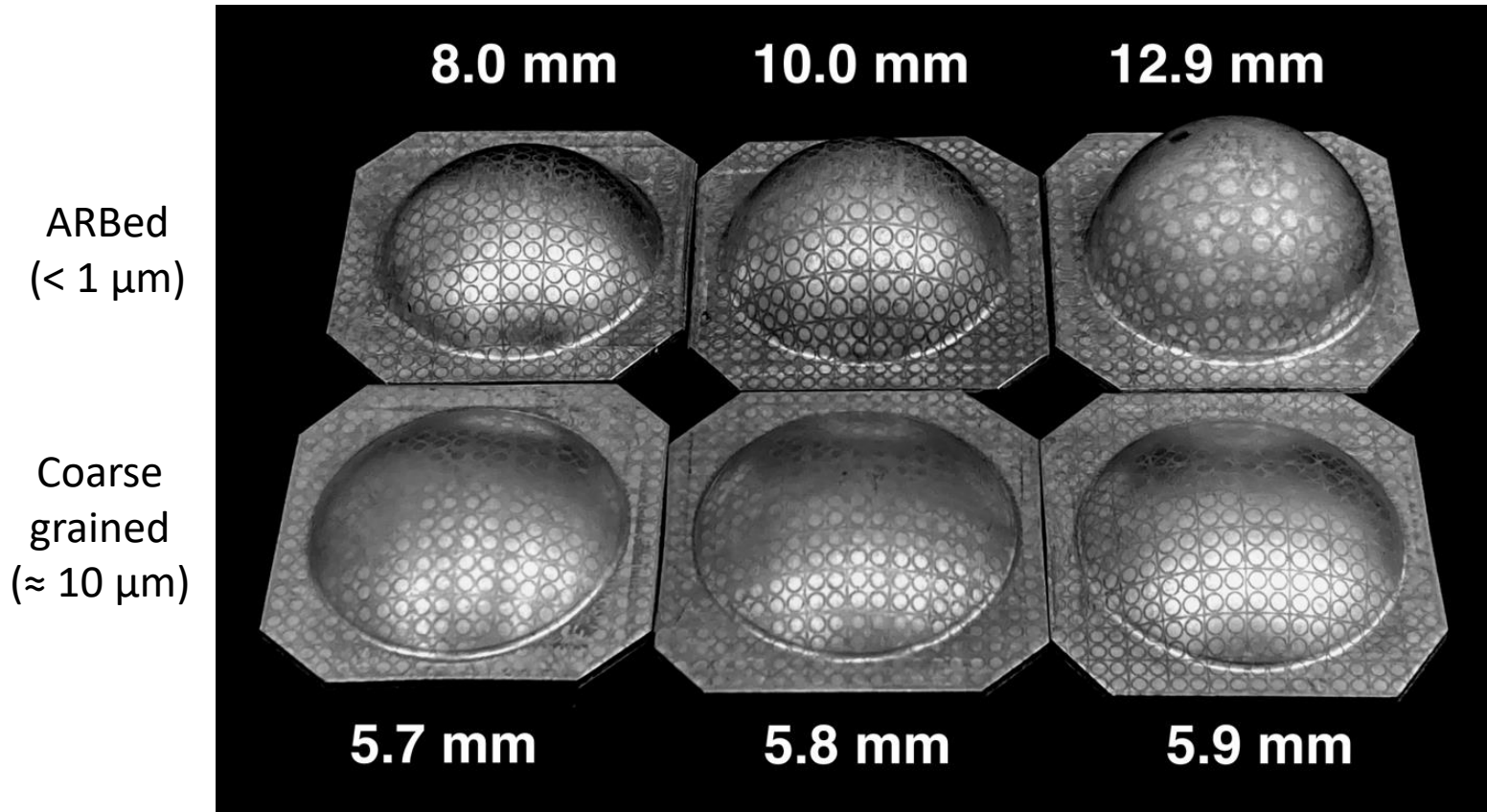


$$P = \frac{4S_0\sigma}{r} \cdot e^{-\dot{\epsilon}t} \sqrt{e^{-\dot{\epsilon}t}(1 - e^{-\dot{\epsilon}t})}$$

Pressure to deform at constant strain rate

# Biaxial Bulge Testing Results

225 °C, 0.0005 s<sup>-1</sup>\*



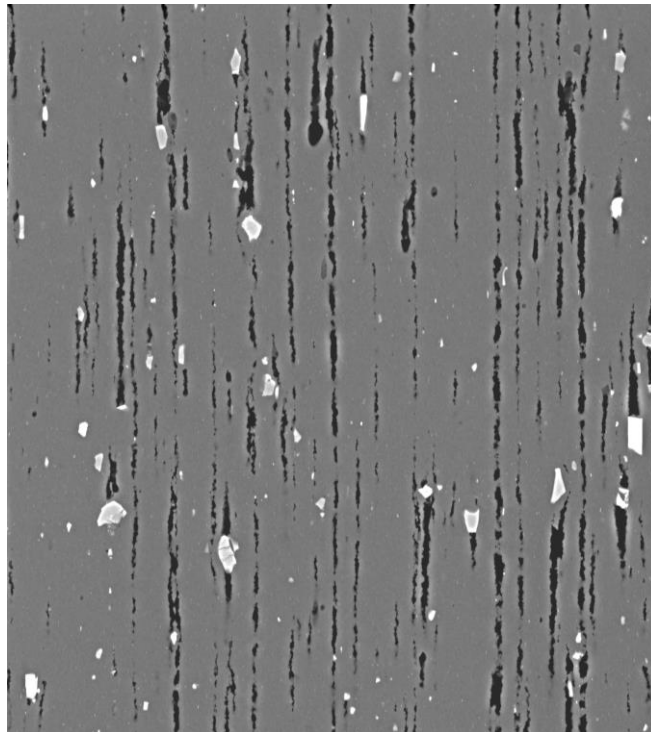
ARBed material demonstrates biaxial superplasticity with:

- 1) lower temperatures
- 2) lower forming pressures

\*strain rates listed are anticipated values, not necessarily observed values

# Comparison of Damage Accumulation

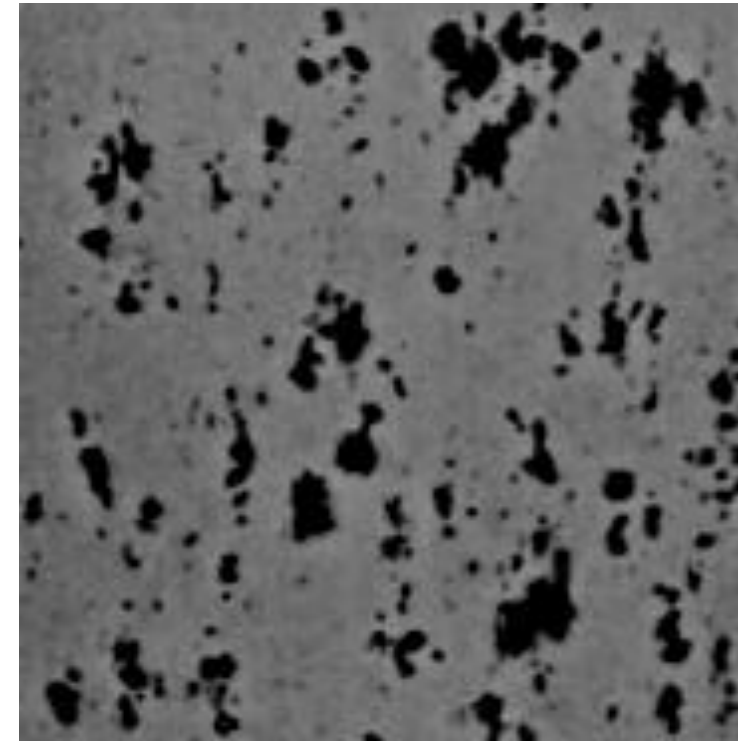
ARBed  
( $< 1 \mu\text{m}$ )  
 $225^\circ\text{C}, 0.0005 \text{ s}^{-1}$



$\epsilon^* = 1.00$

50  $\mu\text{m}$

Coarse  
grained  
( $\approx 10 \mu\text{m}$ )  
 $500^\circ\text{C}, 0.001 \text{ s}^{-1}$



$\epsilon^* = 1.01$

100  $\mu\text{m}$

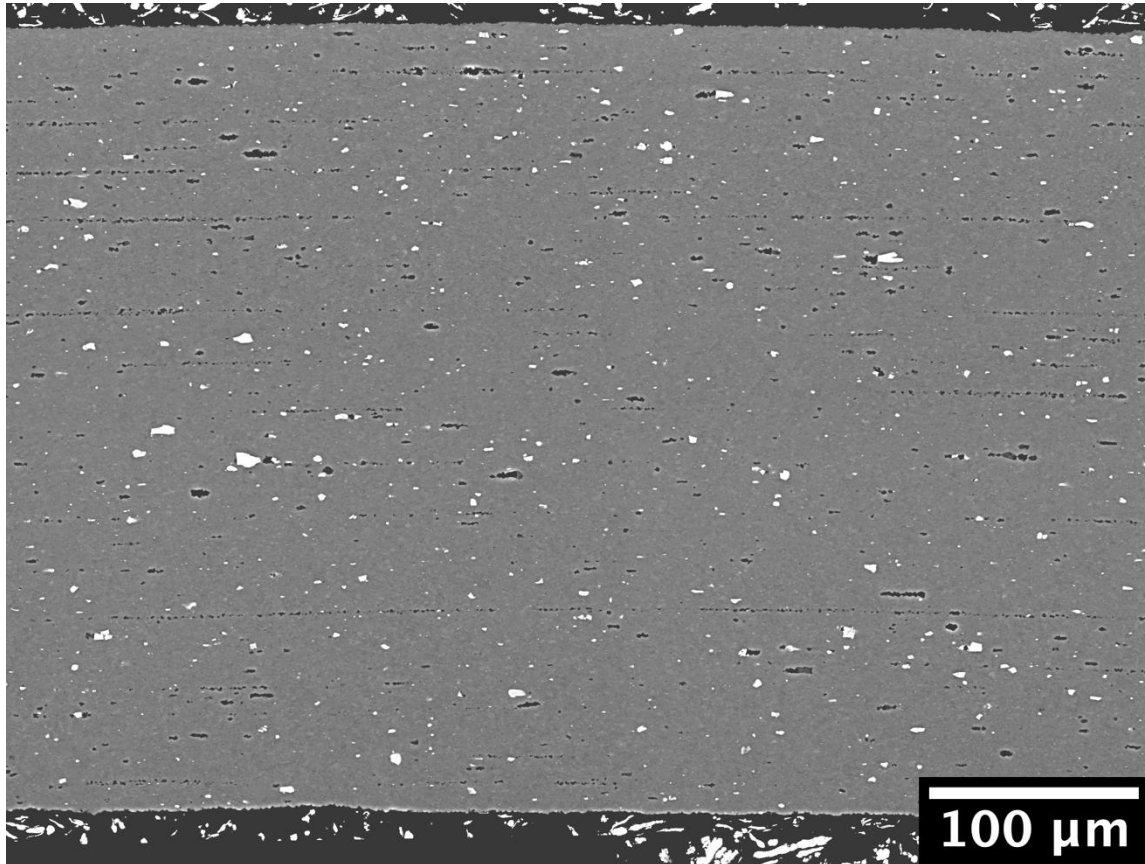
Mean void size  $\approx$  mean grain size

\*tensile strain of bulk sample

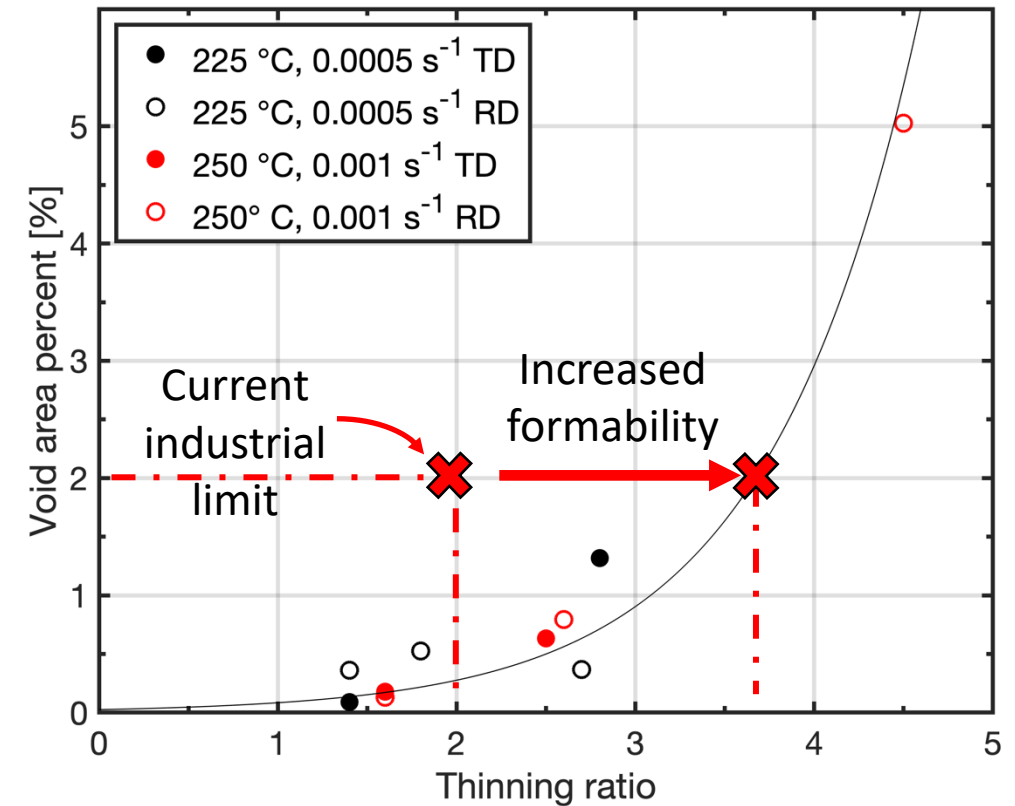


# Formability of ARBed material

250°C, 0.001 s<sup>-1</sup>,  $t_o/t_f = 1.6$

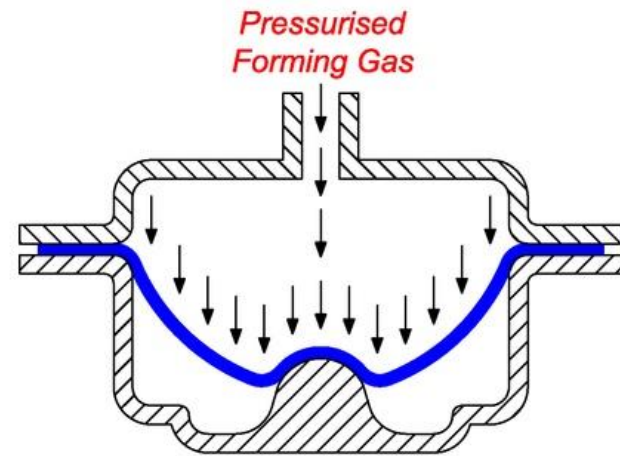
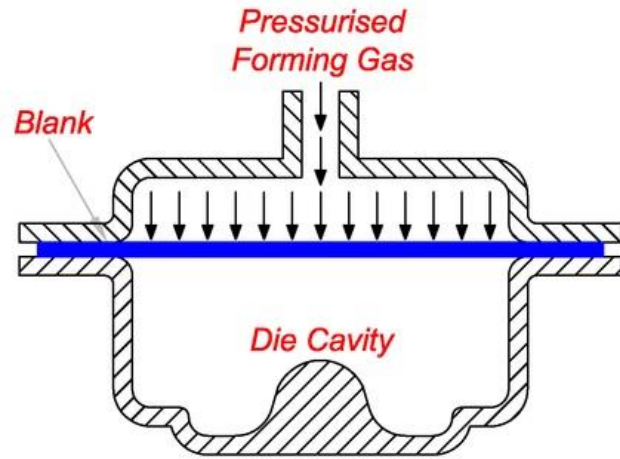


Cross-section along RD at apex of biaxial bulge sample



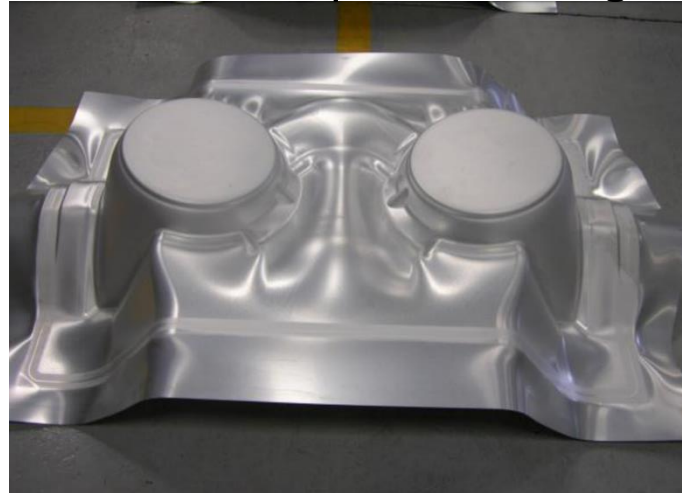
Higher thinning ratios can be achieved with lower void fractions due to smaller void sizes.

# Industrial Relevance: Superplastic Forming



LightMetalAge

Aircraft lamp can housing



Barnes et al., *Mat. Sci. Forum*, 2003.

2018 Bentley Continental GT



LightMetalAge

ARB processed 5083:

Grain size: ~~10~~  $\mu\text{m}$  **1  $\mu\text{m}$**

Temperature: ~~500~~  $^{\circ}\text{C}$  **225  $^{\circ}\text{C}$**

Strain rates:  $1 \times 10^{-3} \text{ s}^{-1}$

Thinning ratios: ~~2.0~~ **3.5**

Void fraction: 2%

# Thank You!

Brady McBride

[brady.mcbride@atimetals.com](mailto:brady.mcbride@atimetals.com)

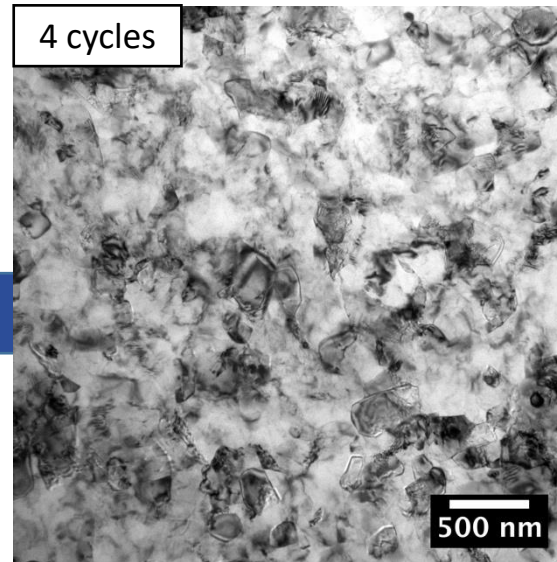
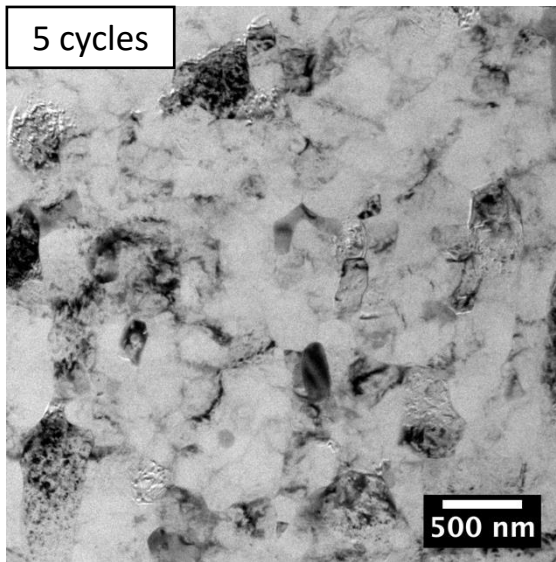
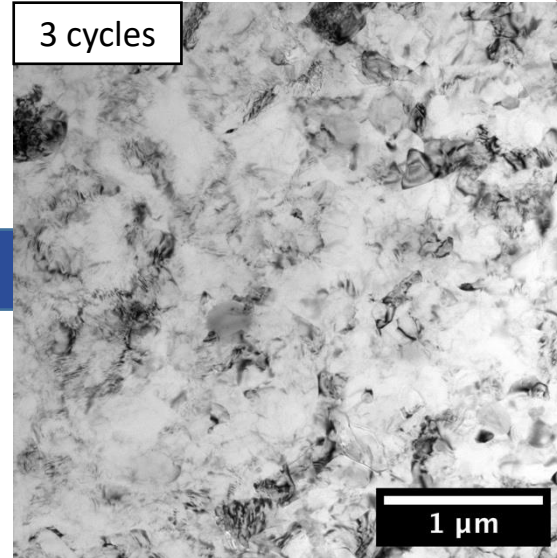
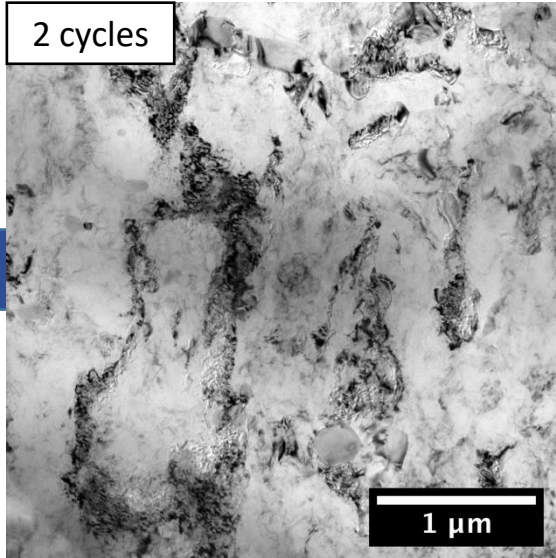
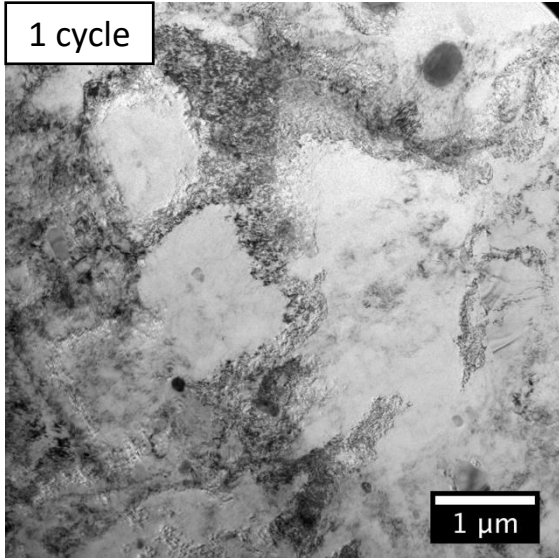
Colorado School of Mines (former)

ATI Specialty Materials (current)

# Supplemental Slides

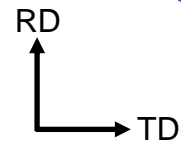


# Grain Refinement (Brightfield TEM)



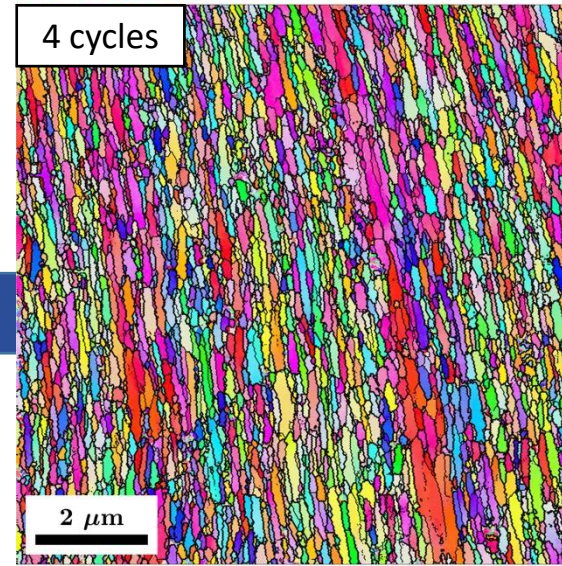
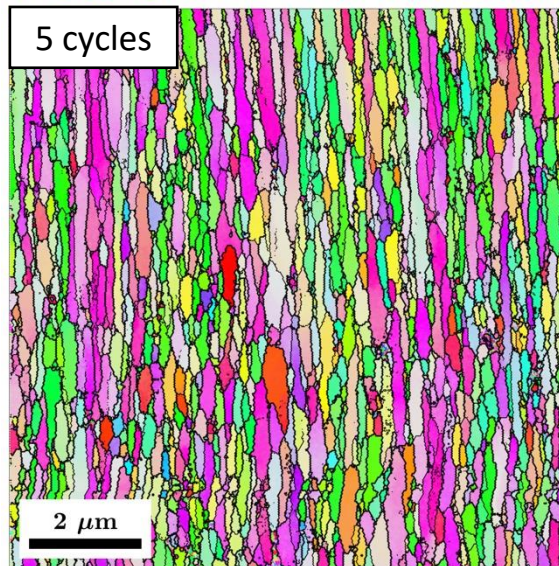
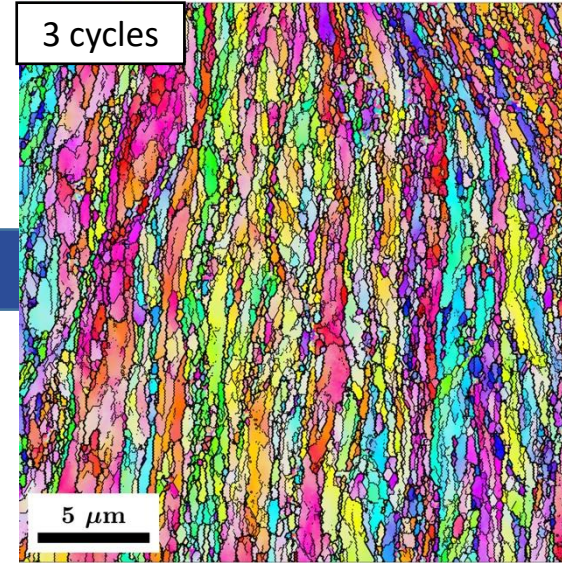
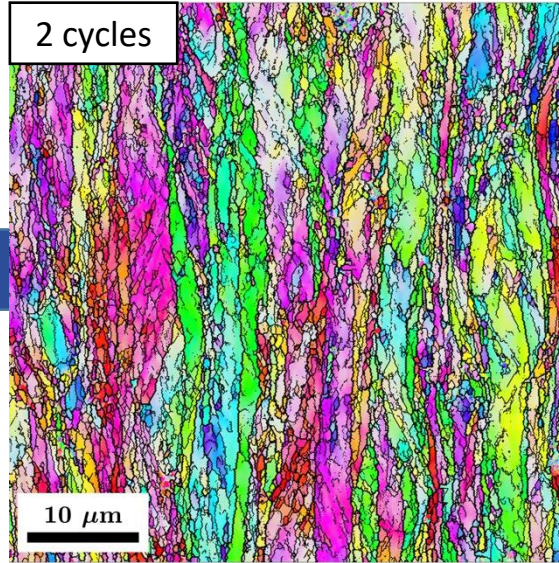
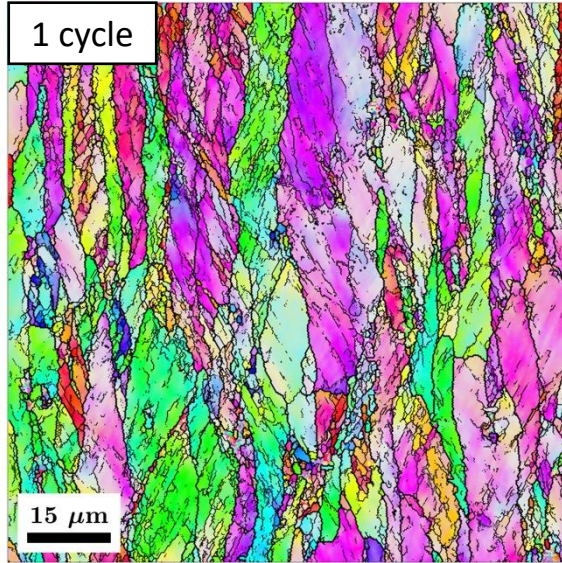
Grain subdivision, rotation and dislocation conglomeration lead to grain refinement (*"in-situ" recrystallization*)

\*observed at random location through-thickness



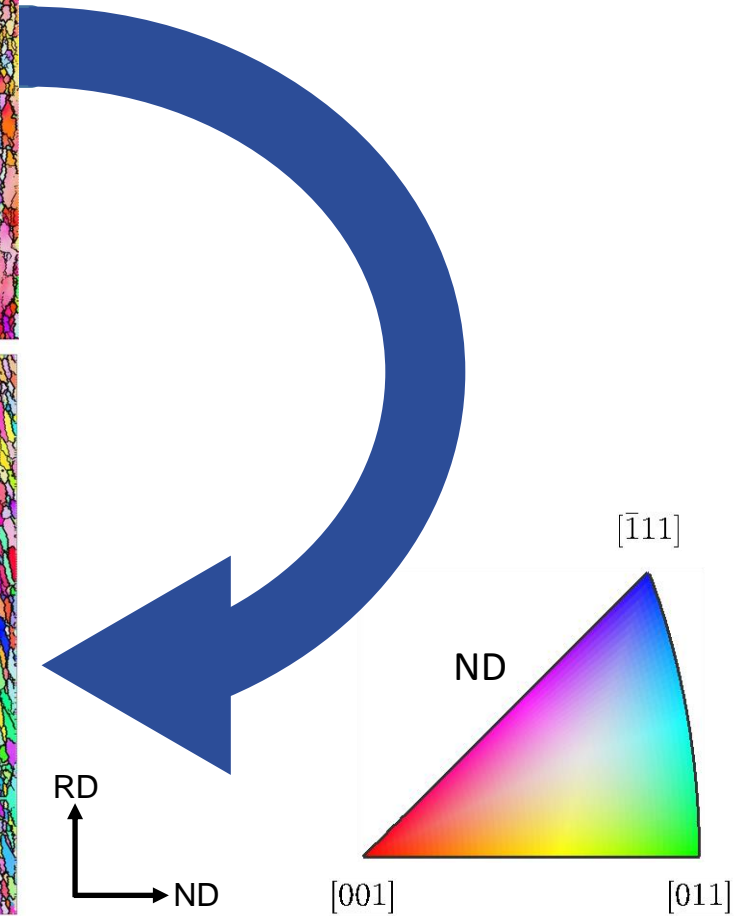


# Grain Refinement (Inverse pole figure maps)



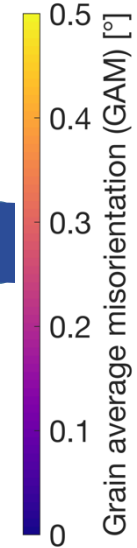
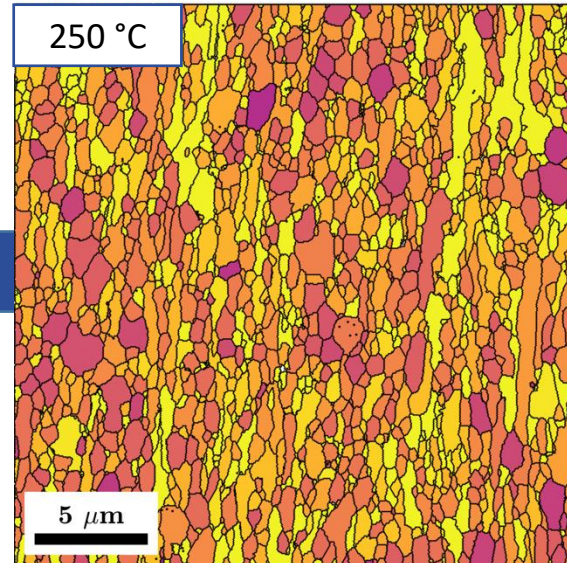
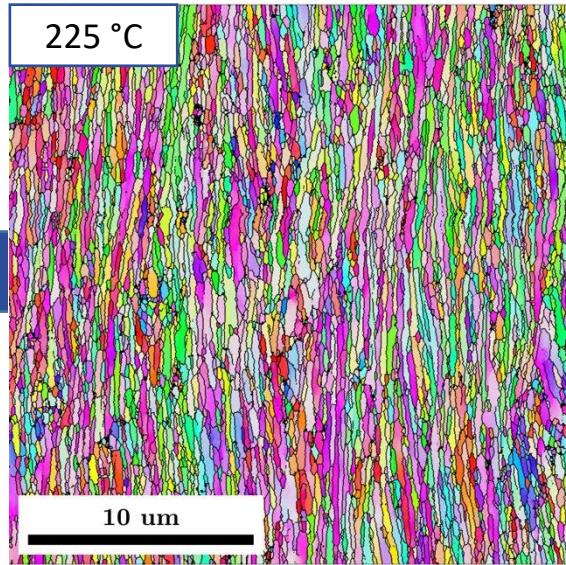
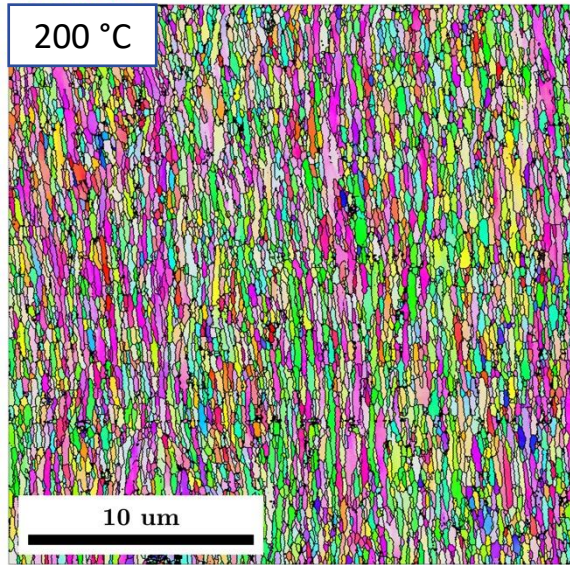
Grain subdivision  
and rotation  
lead to grain refinement

\*observed in the vicinity of  
the centerline bond

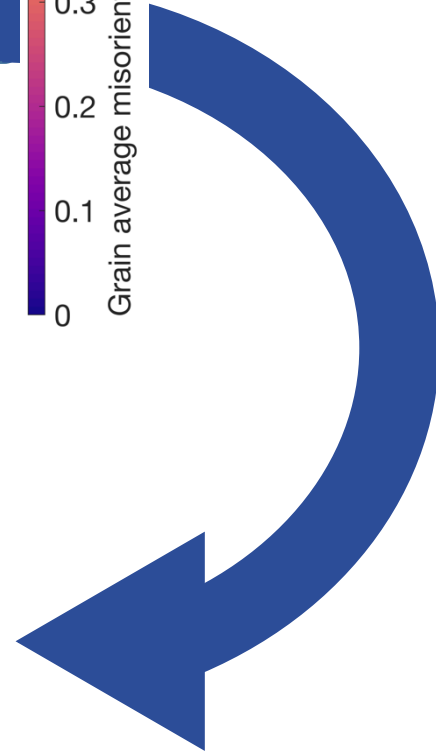
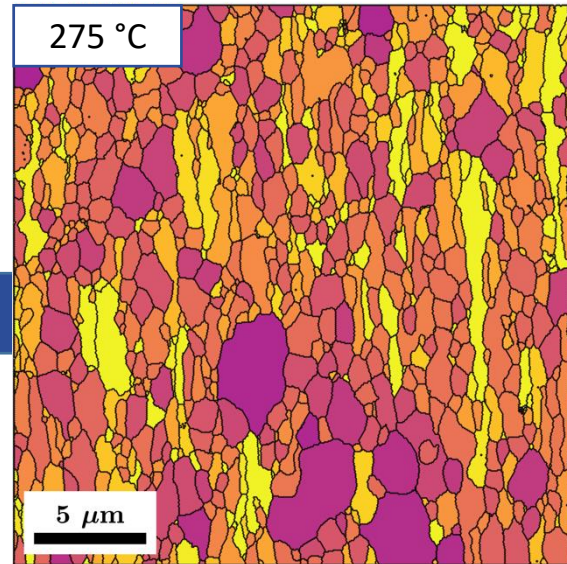
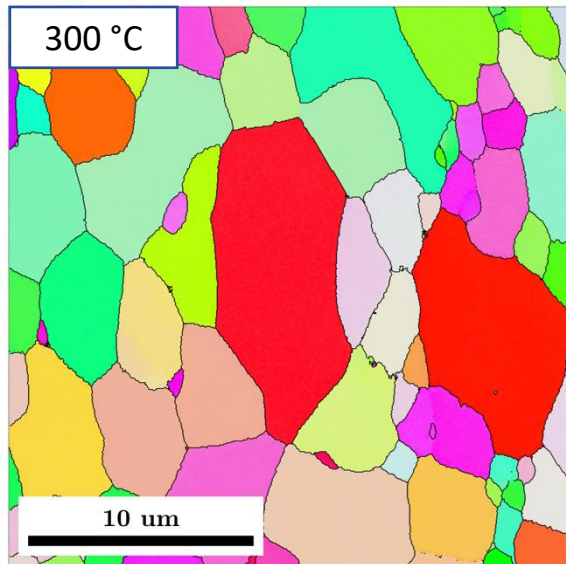
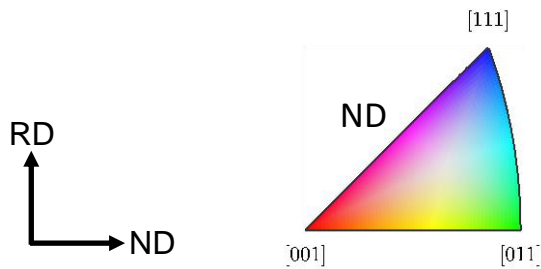




# 15 minute Static Annealing Trials (EBSD)

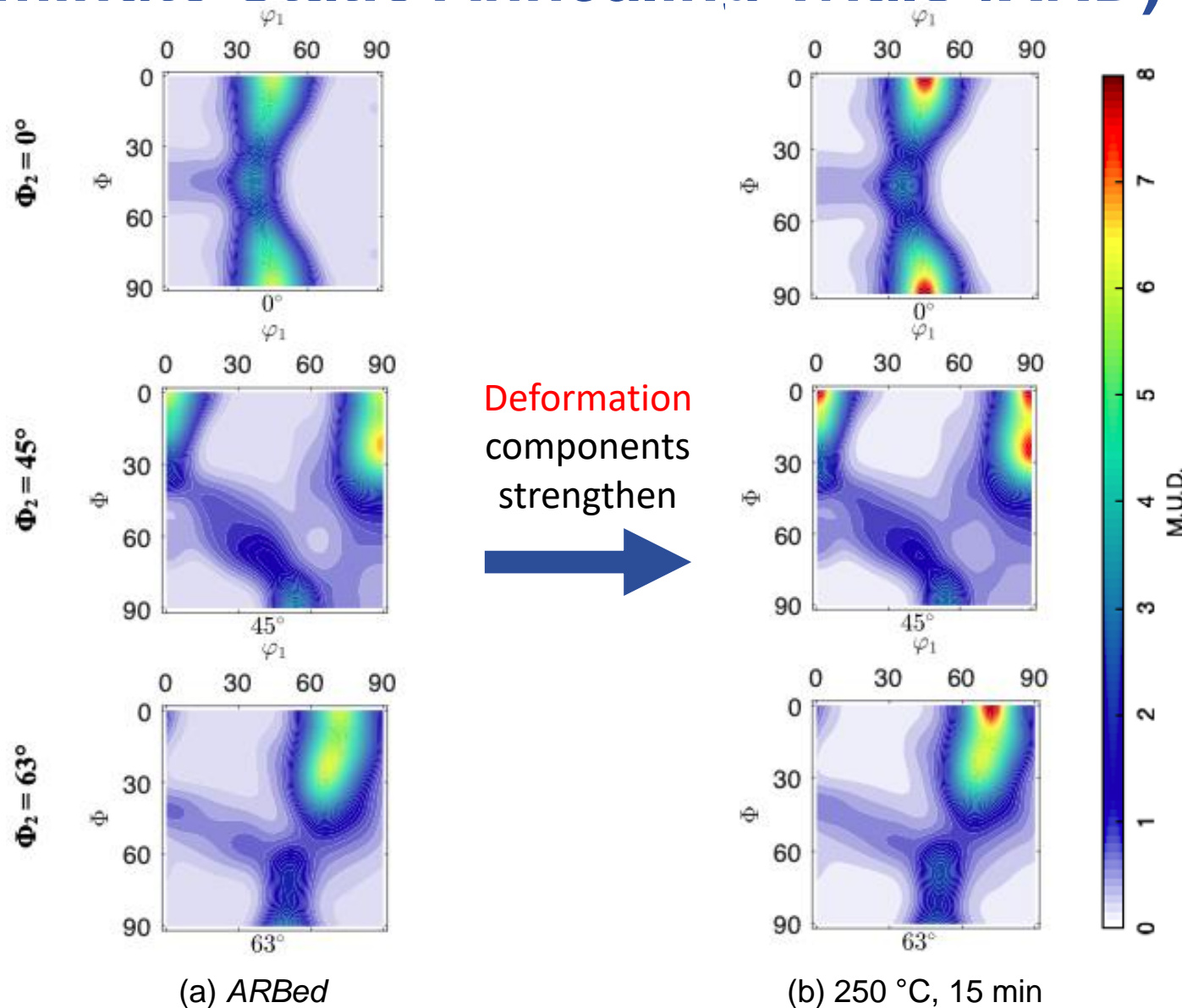


*Gradual* reduction in strain energy (GAM) throughout microstructure



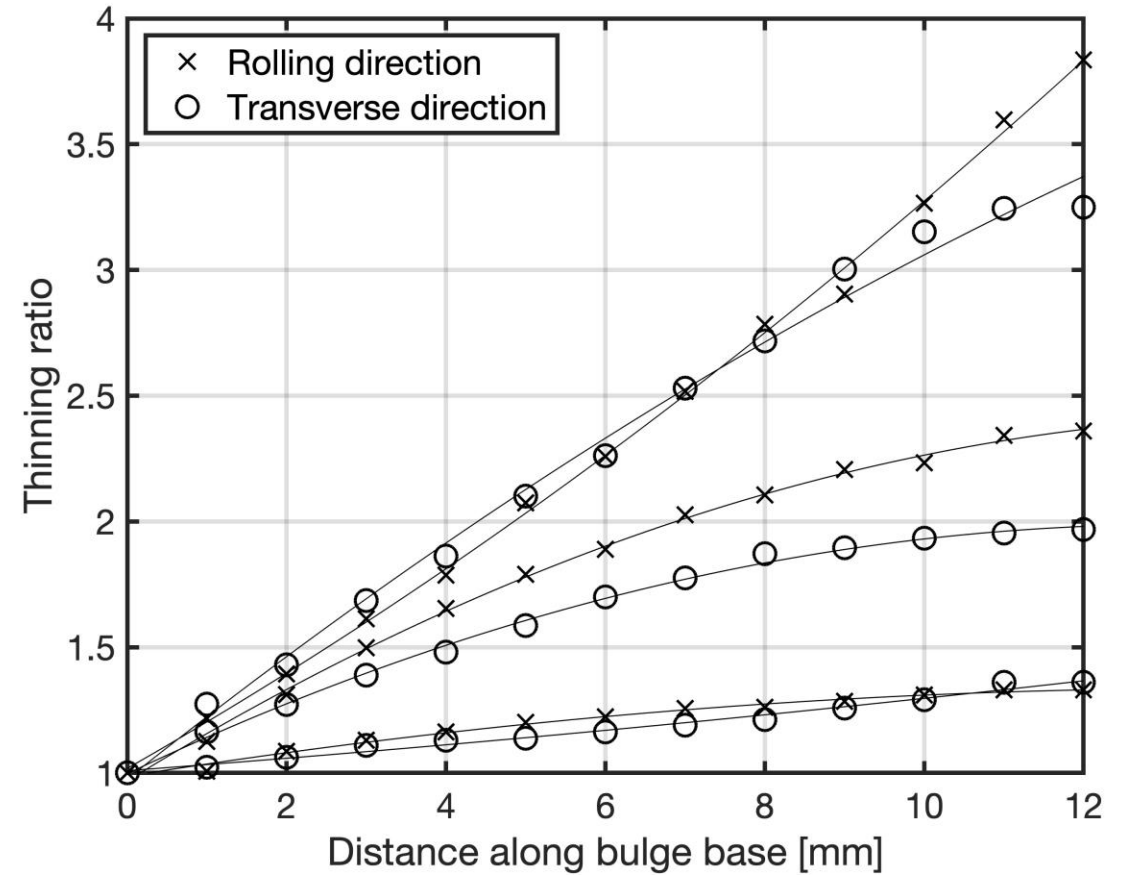
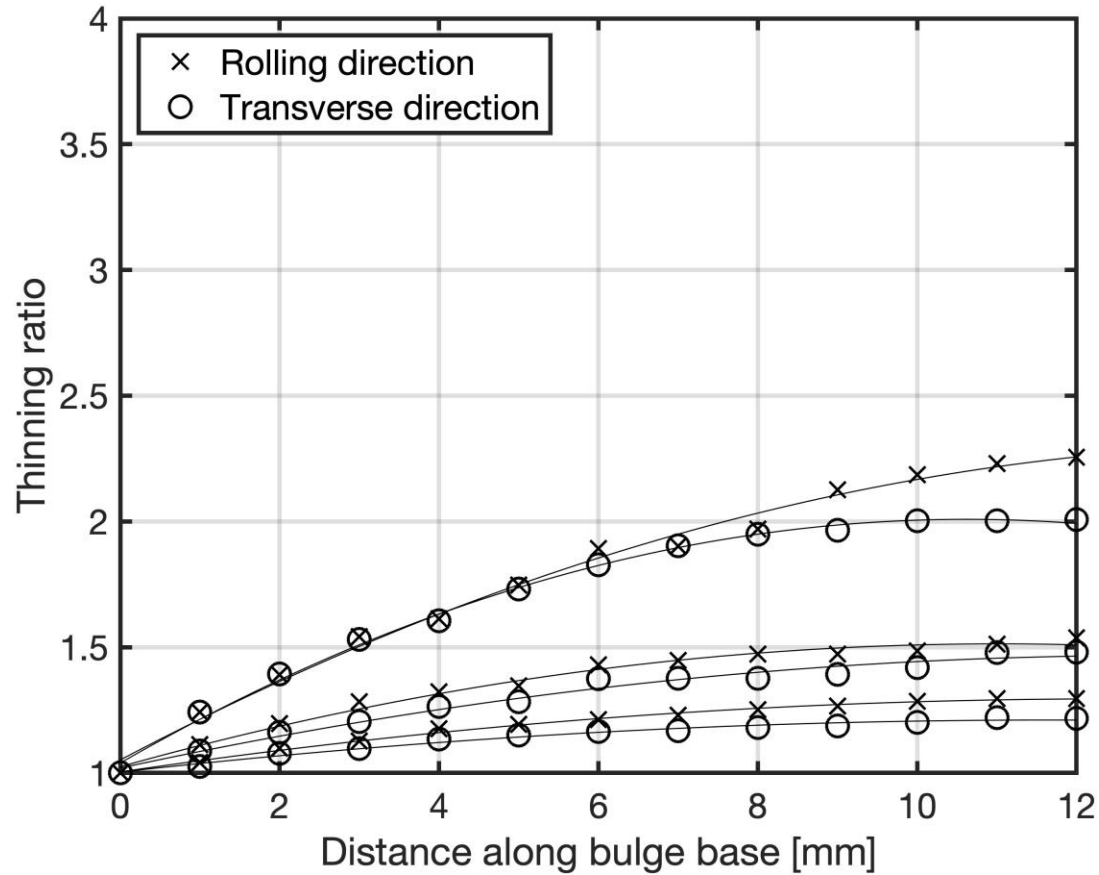


# 15 minute Static Annealing Trials (XRD)

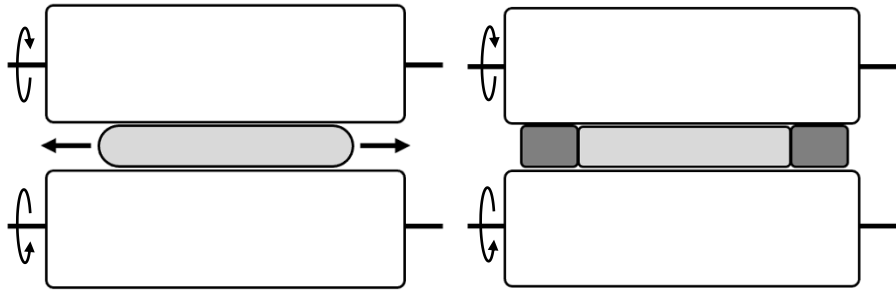


Annealing reduces  
intragranular orientation gradients  
leading to  
texture strengthening

# Thinning Ratios

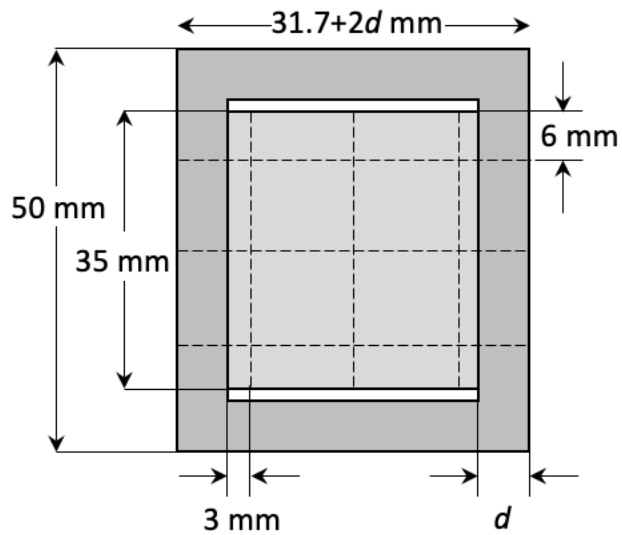


# Mitigation of Edge Cracking

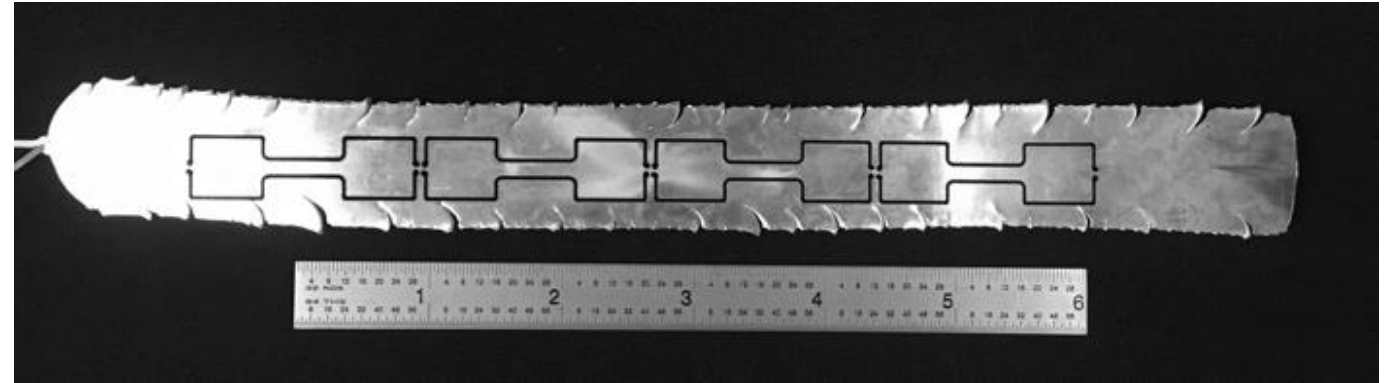


Lateral spreading  
leads to  
edge cracking

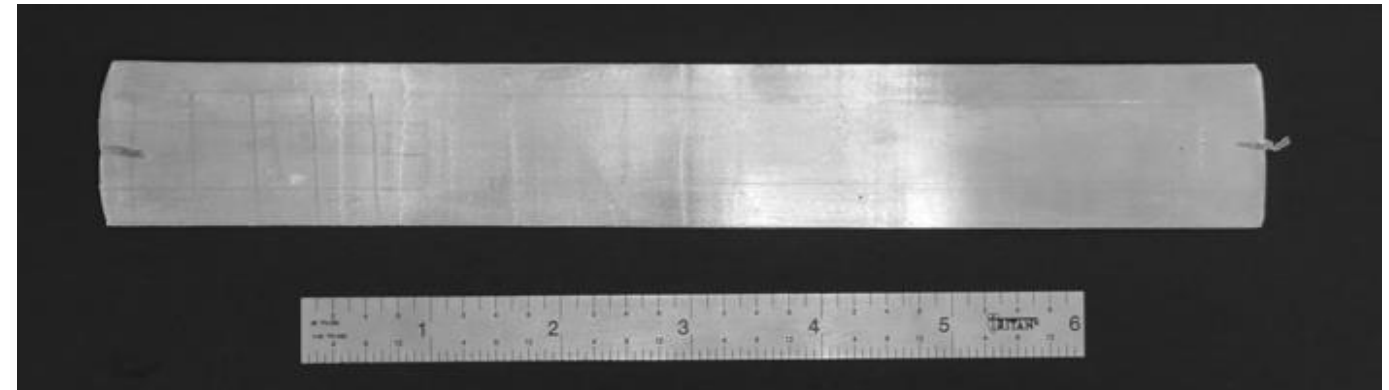
Lateral constraint  
reduces  
lateral spreading



5083 5 ARB – No Constraint



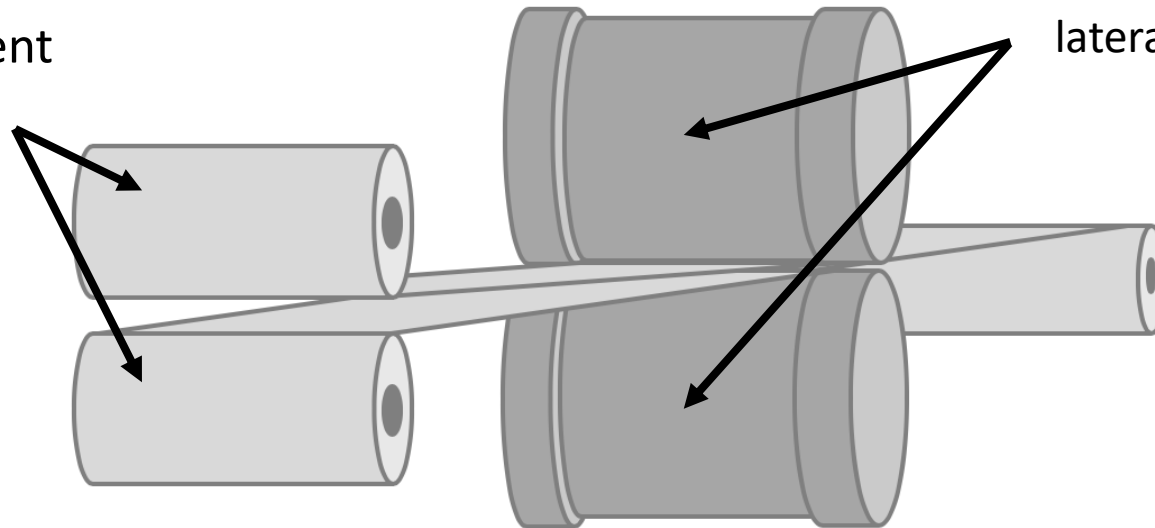
5083 5 ARB – 6 mm Constraint



McBride et al., J. Manu. Proc., 2010.

# Scaling for Industry

Tensioned uncoiler  
aides in sheet  
alignment



Machined channel  
in rolls provides  
lateral constraint

# 100-ton Fenn Rolling Mill



133 mm (5.25") cold rolls  
100,000 lb capacity  
37 RPM single speed

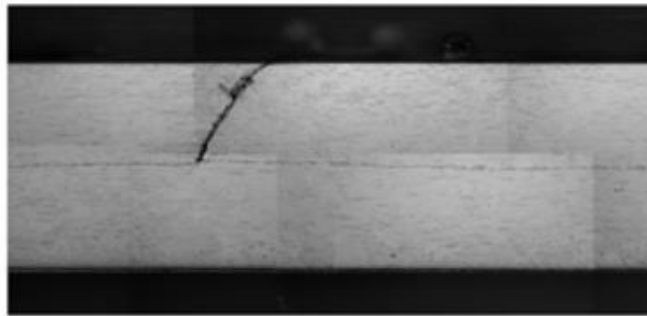
Configurable for:  
4-high cold rolling  
Hot rolling (200 °C)  
Rod rolling (25 mm to 10 mm)



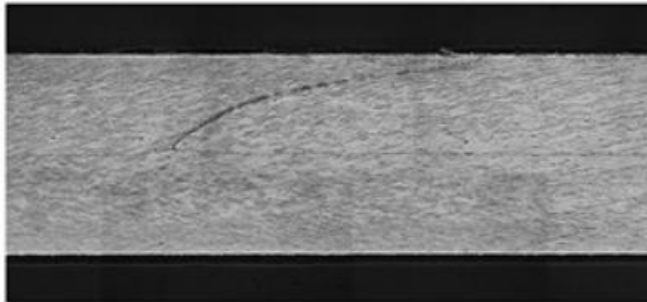
# How is ARB Processing Different from Conventional Rolling?

## 1. Redundant shear

With lubrication



Without lubrication



ND  
↑  
RD  
→

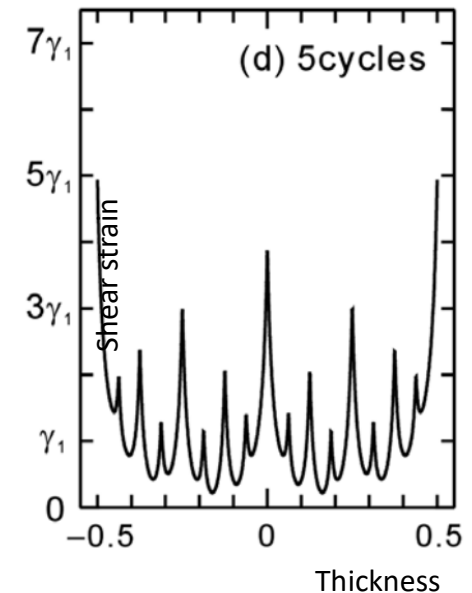
1mm

## 2. Consistent, through-thickness deformation

To obtain  $\epsilon = 4.0$ , 96.9 % reduction:

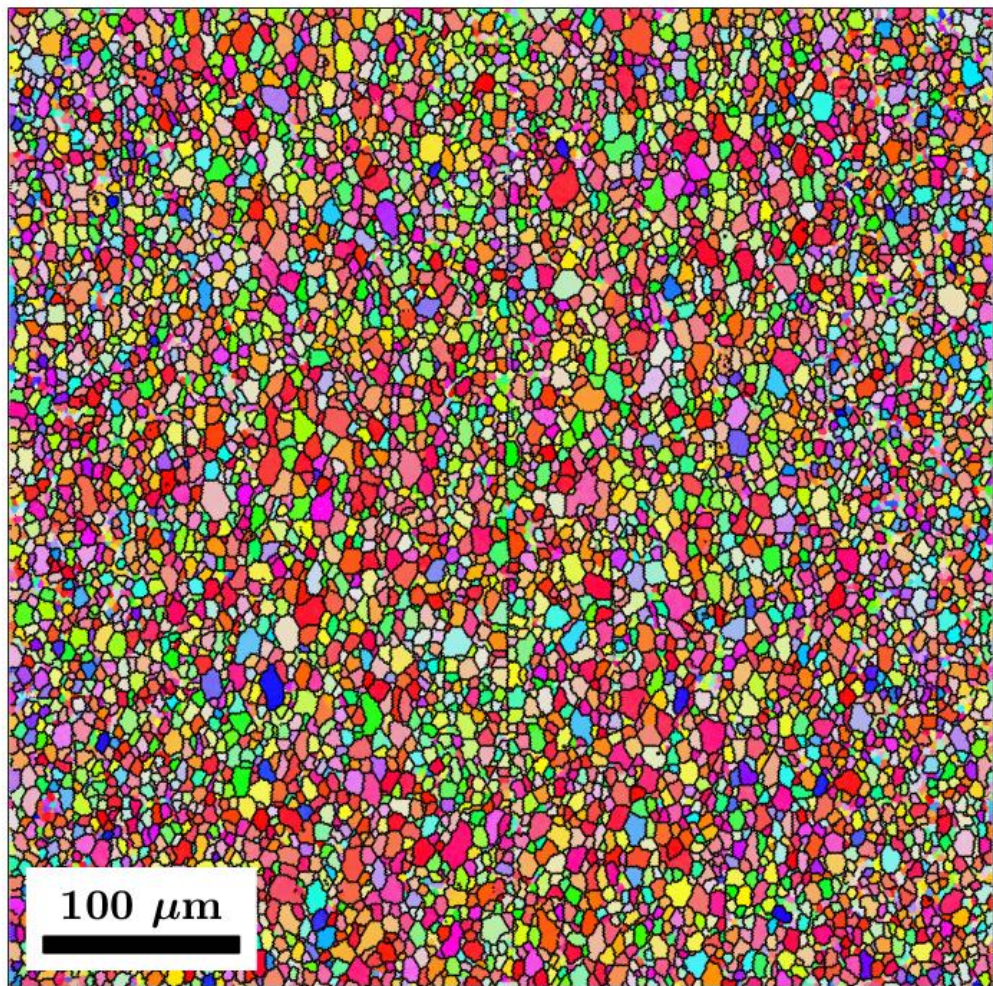
<u>5 ARB cycles</u> (2x) 1 mm sheets ↓ (1x) 1 mm sheet	<u>Convention rolling</u> 32.5 mm plate ↓ 1 mm sheet
---	---

## 3. Introduction of shear through-thickness



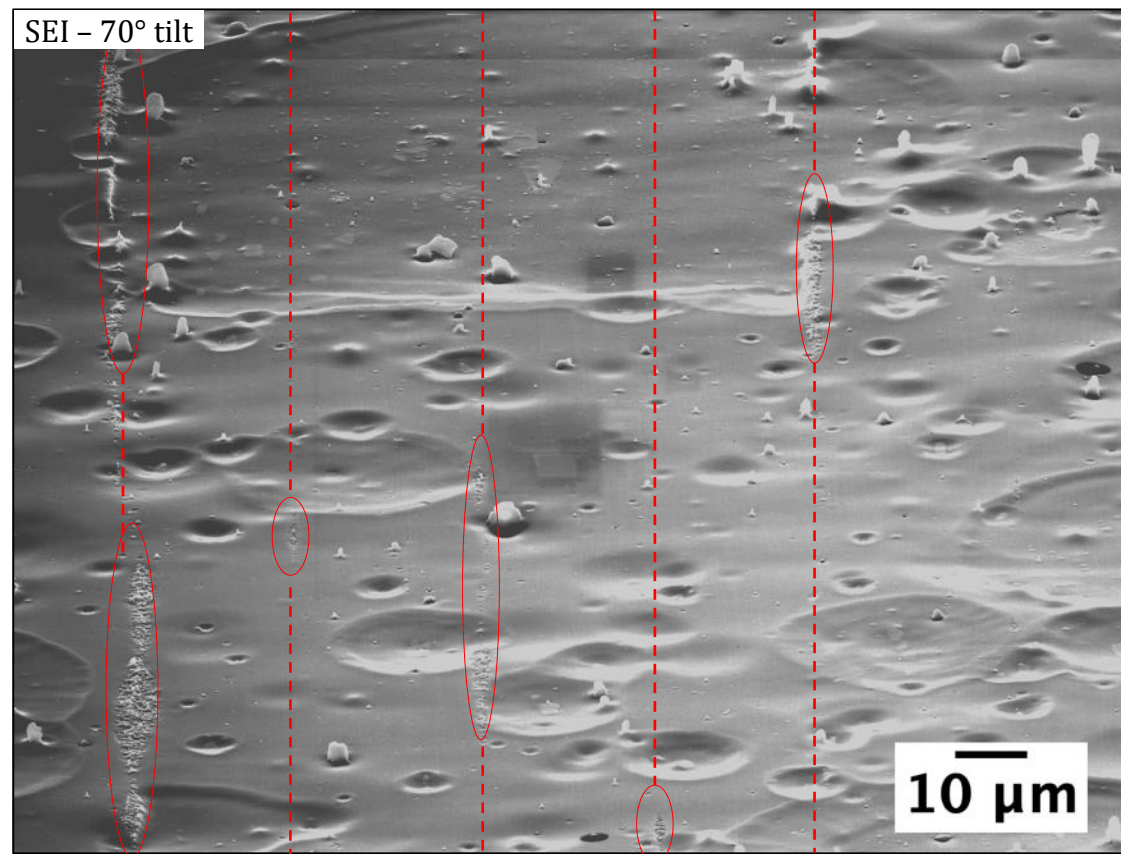
# Recrystallized Microstructure after ARB Processing

Recrystallization does not seem to occur across bonding interfaces



RD  
ND

5 ARB cycles + 500 °C, 30 min



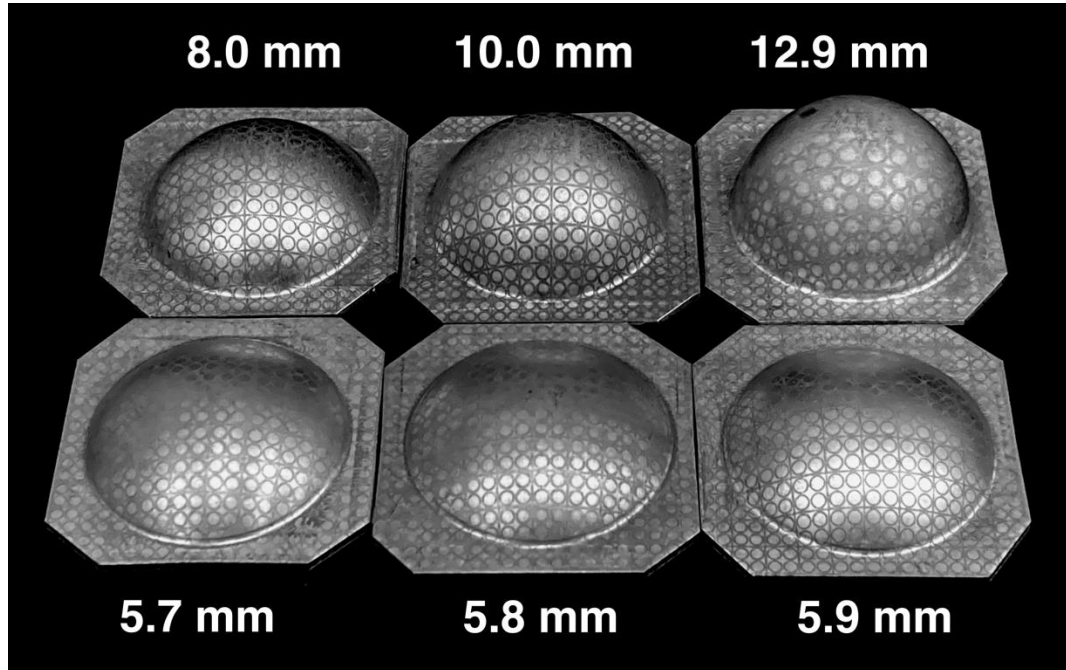
RD  
ND

5 ARB cycles



# Biaxial Bulge Testing: Results

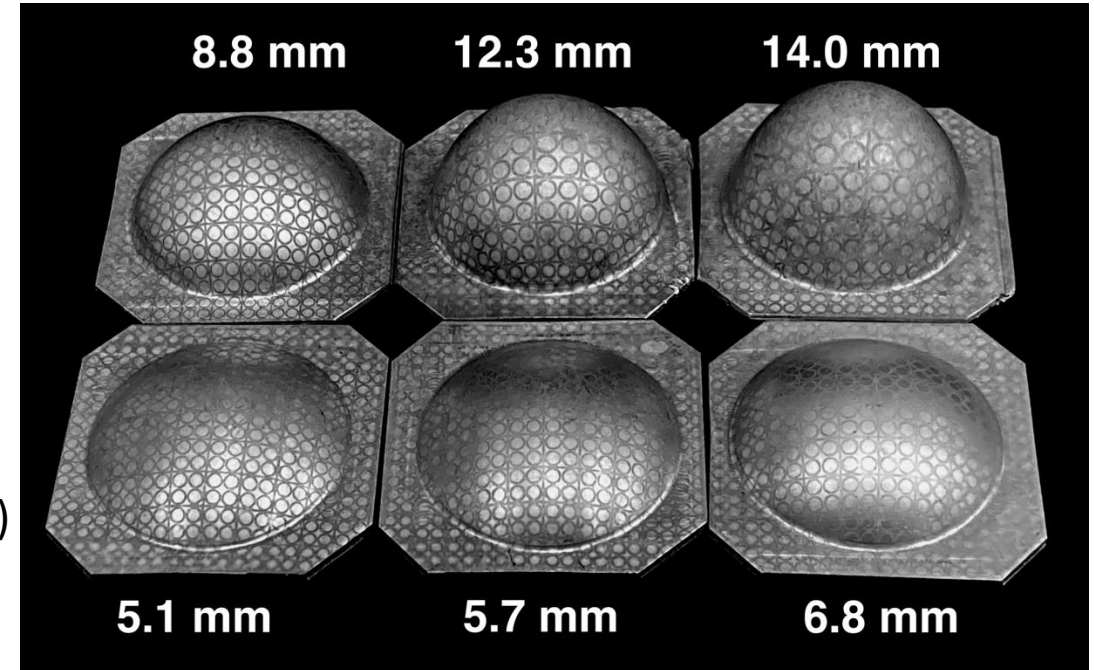
225 °C, 0.0005 s<sup>-1</sup>\*



ARBed  
( $< 1 \mu\text{m}$ )

Coarse  
grained  
( $\approx 10 \mu\text{m}$ )

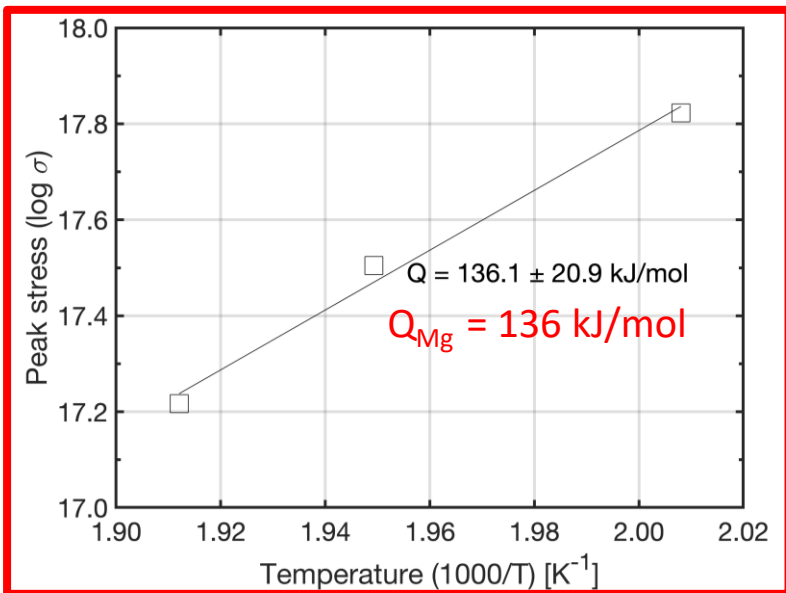
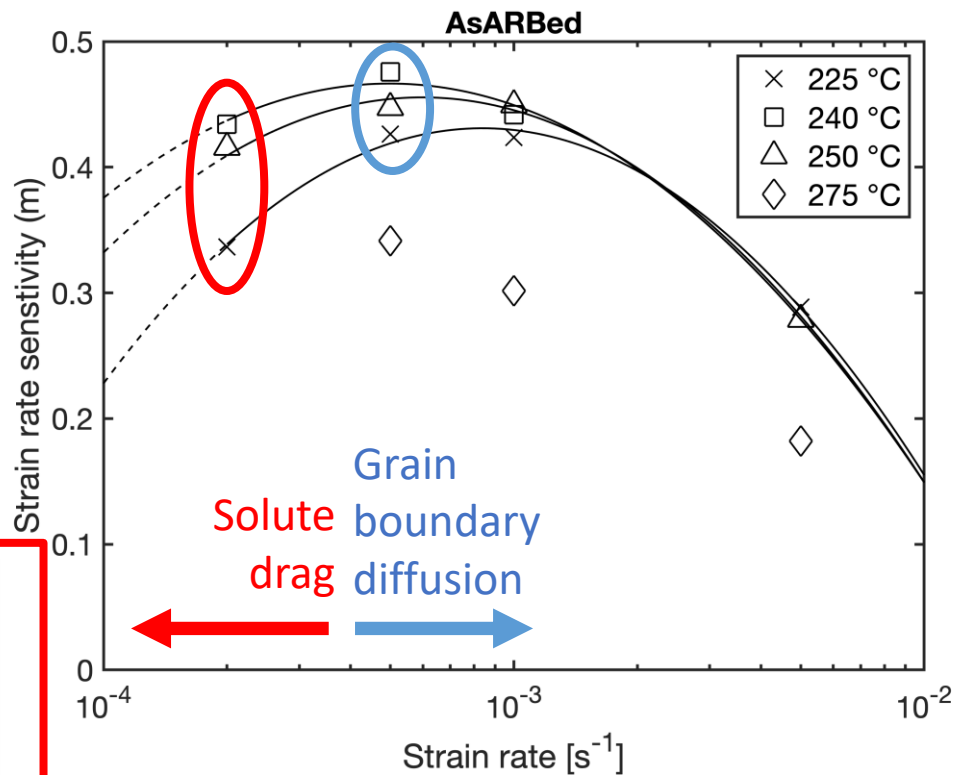
250 °C, 0.001 s<sup>-1</sup>\*



ARBed material exhibits biaxial superplasticity  
with **lower temperatures** and **lower forming pressures**

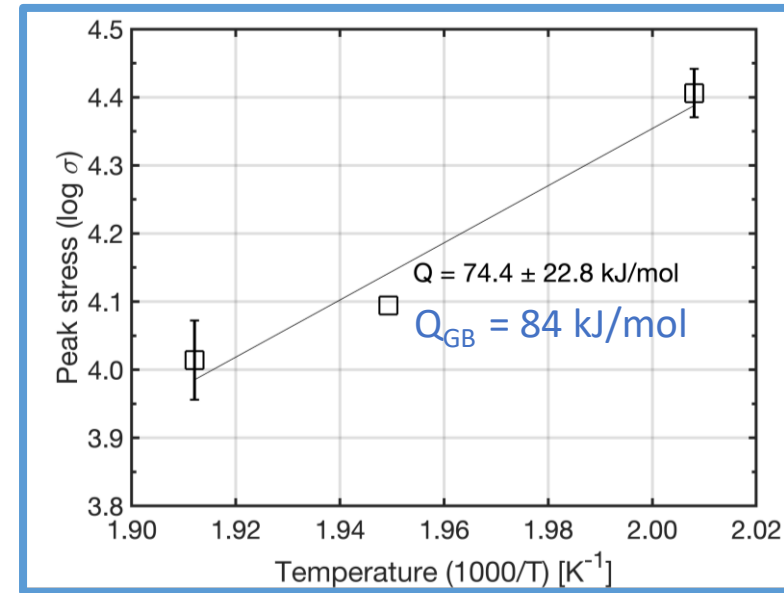
\*strain rates listed are anticipated values, not necessarily observed values

# Identifying Strain Rate and Temperature Limits



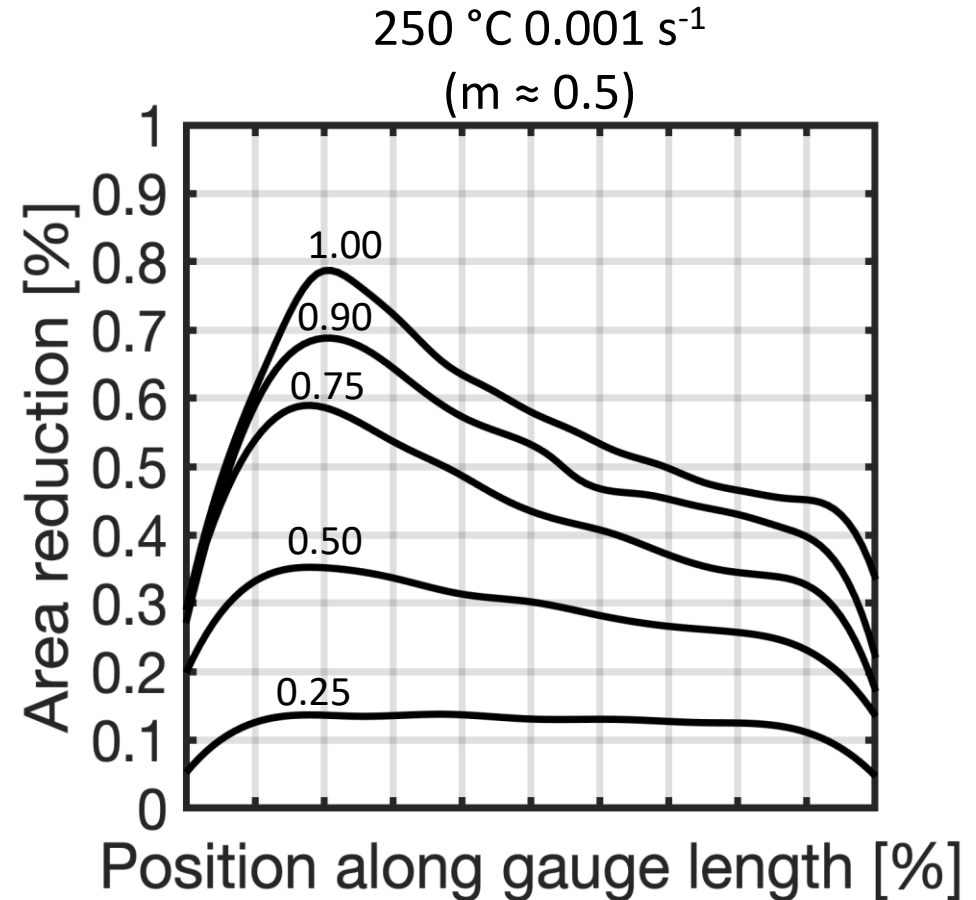
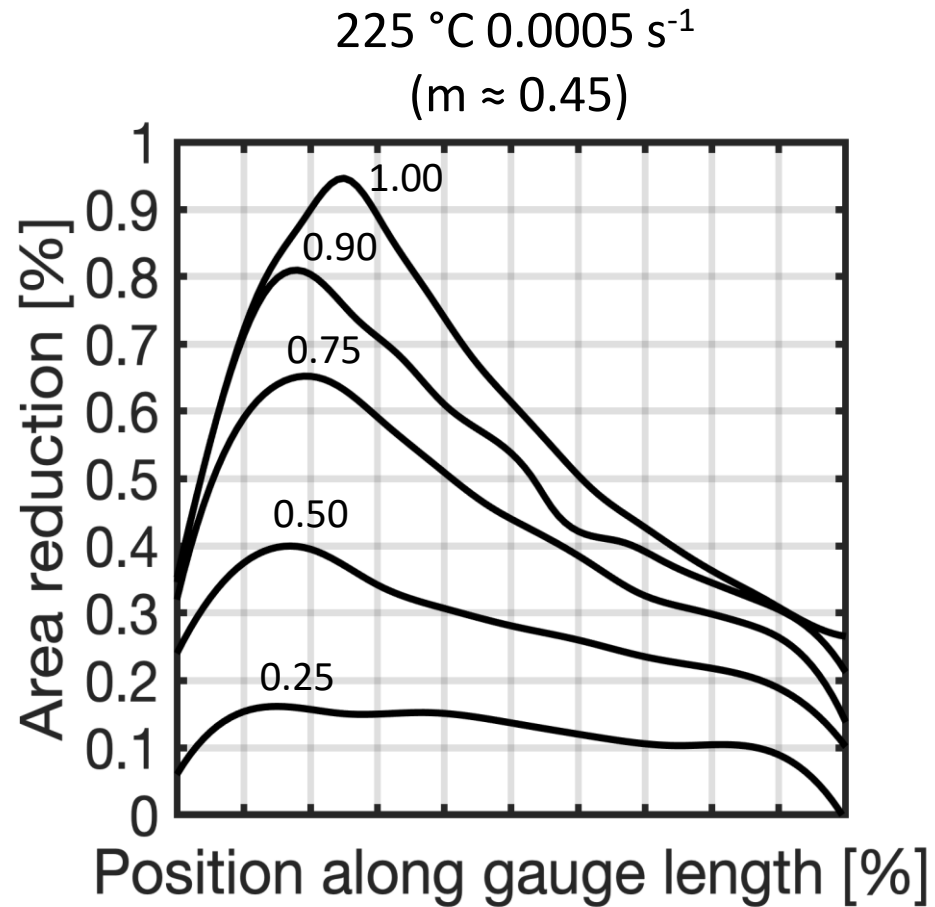
Activation energy for deformation

$$Q = \frac{k \delta \ln \sigma}{m \delta 1/T} \Big|_{\epsilon, \dot{\epsilon}, d}$$





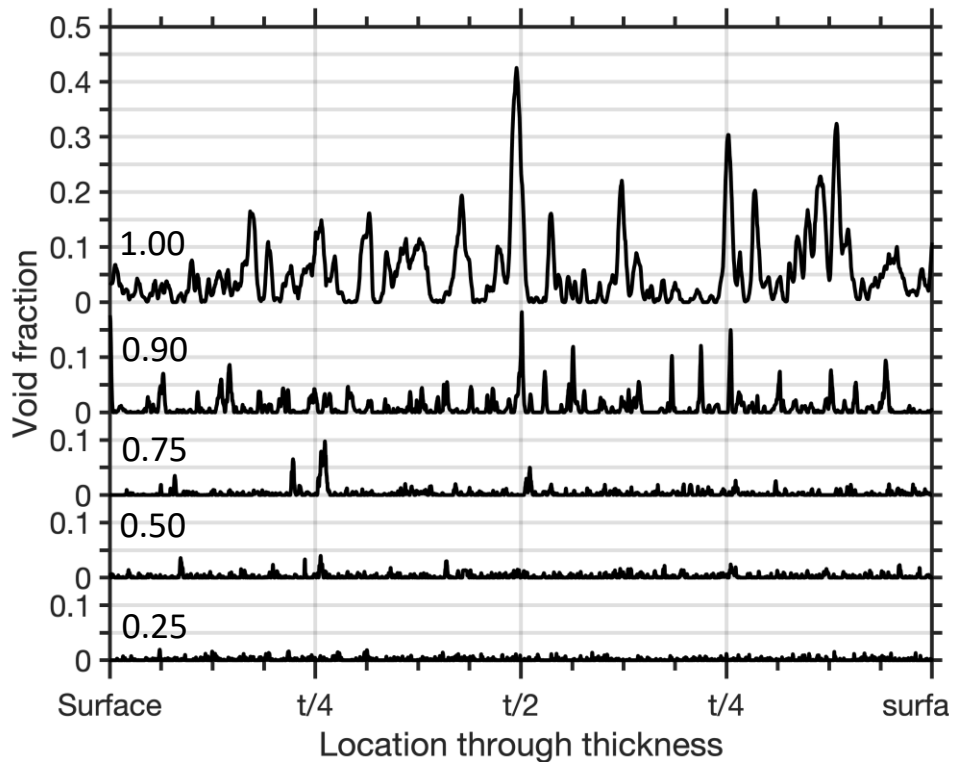
# Strain Uniformity During Deformation



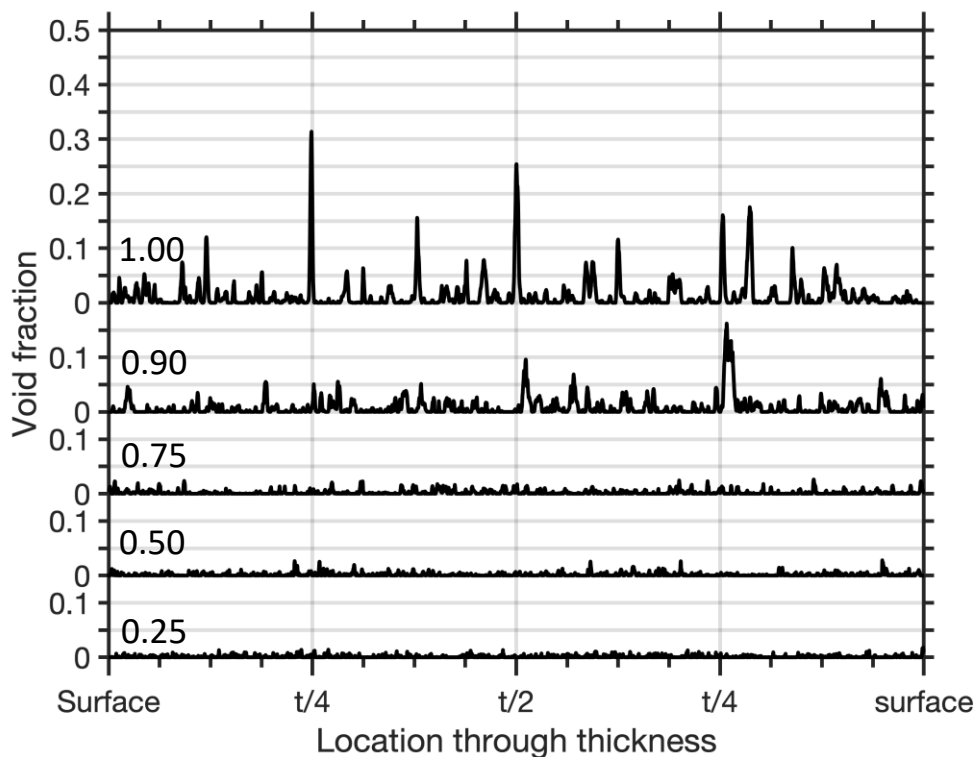
Significant strain localization after  $\epsilon = 0.75$  ( $e = 1.10$ )

# Damage Accumulation

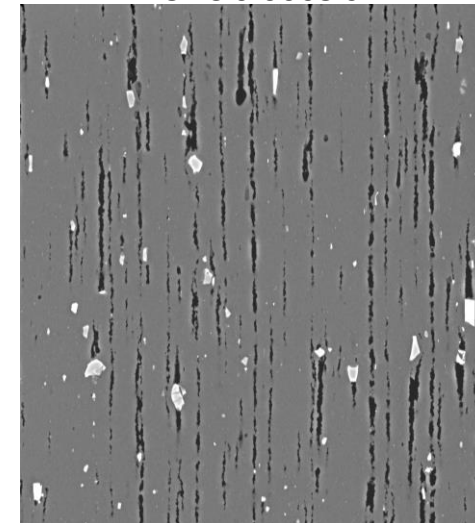
225 °C 0.0005 s<sup>-1</sup>



250 °C 0.001 s<sup>-1</sup>



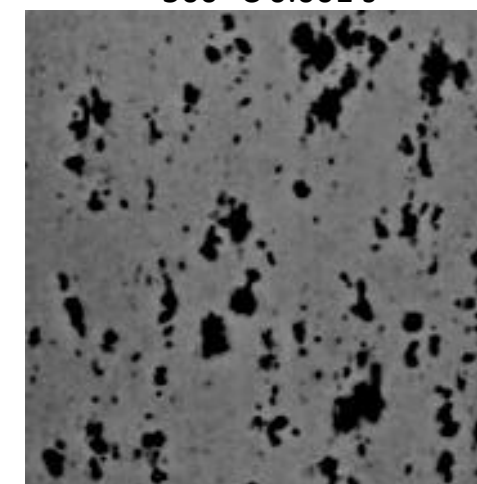
225 °C 0.0005 s<sup>-1</sup>



$\epsilon = 1.00$

50  $\mu\text{m}$

500 °C 0.001 s<sup>-1</sup>

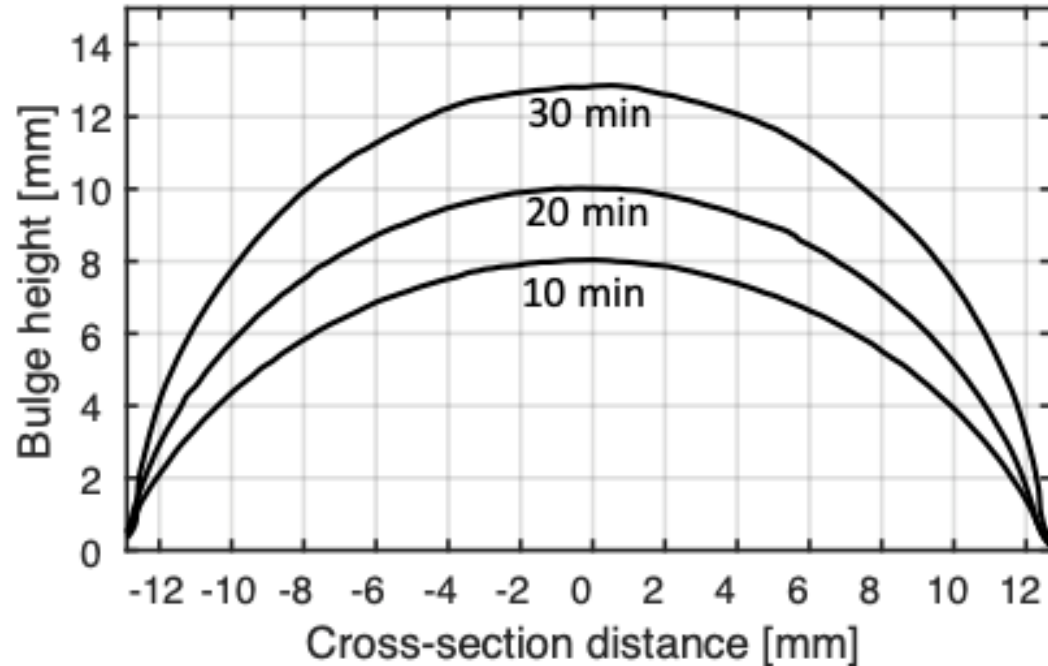


$\epsilon = 1.01$

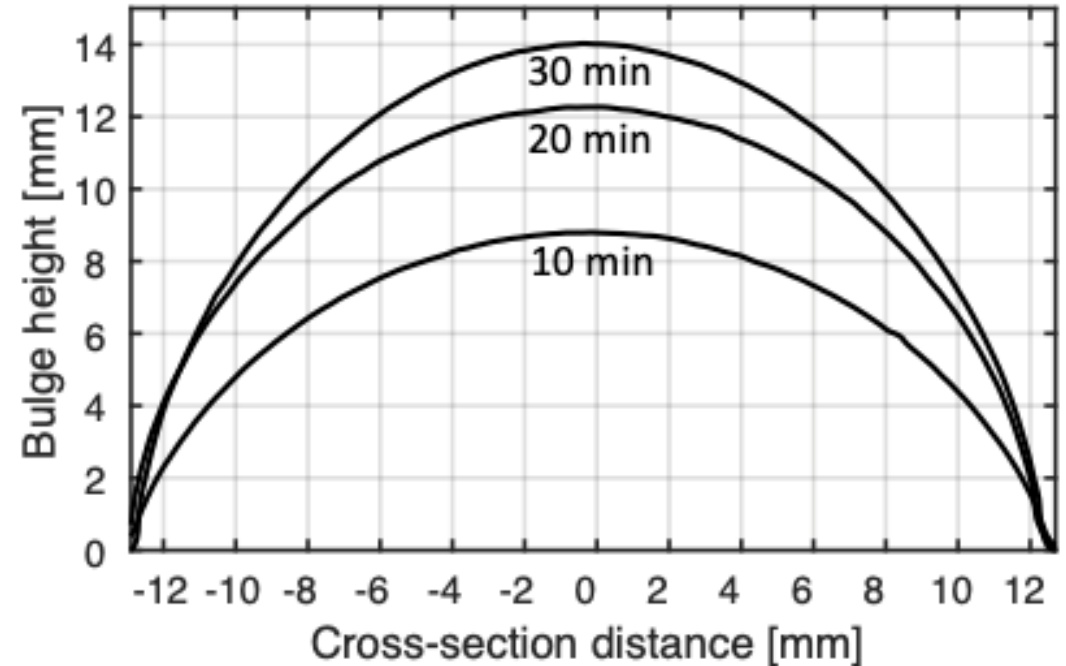
100  $\mu\text{m}$

**Significant** strain-induced void growth (voids > 1  $\mu\text{m}$ ) for  $\epsilon > 0.75$  ( $e > 1.1$ )

# Analysis of Bulge Test Specimens



Height and  
thickness profiles

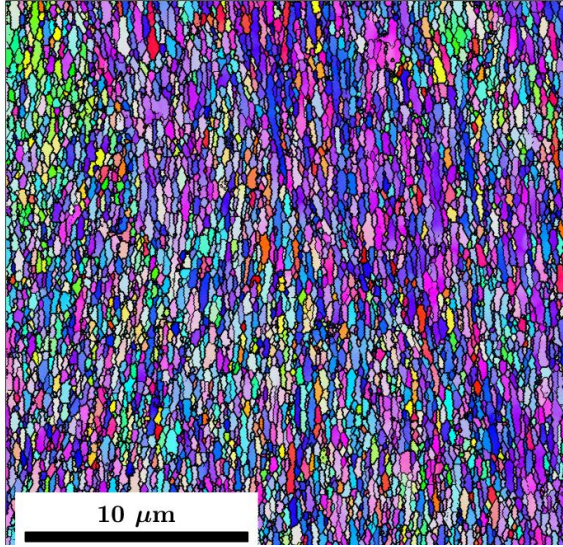


Analytical models for  
superplastic forming

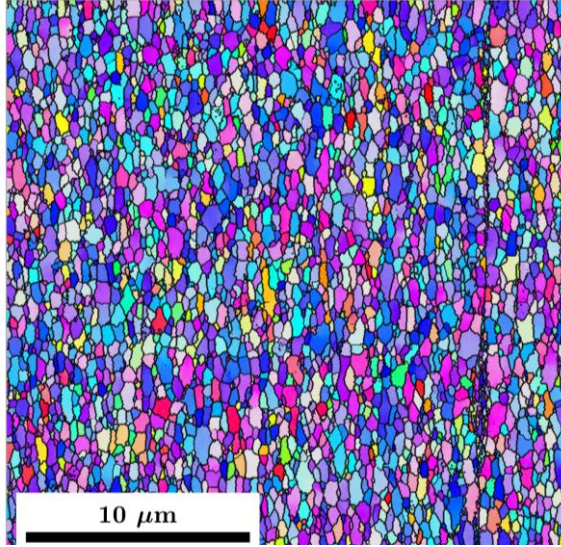


# Incremental strain at 225 °C, 0.0005 s<sup>-1</sup>

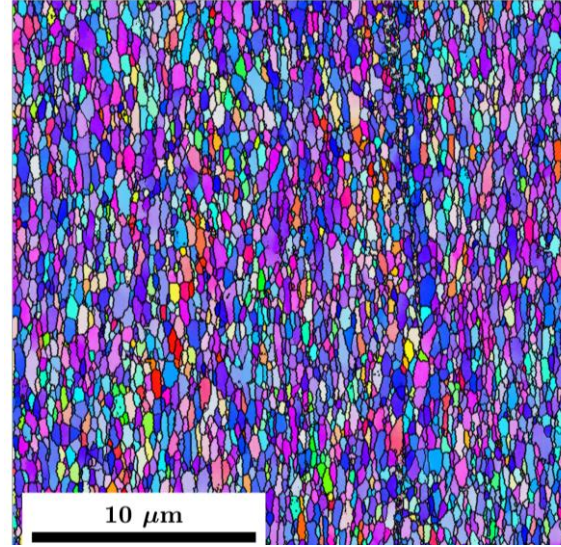
$\epsilon = 0.1, 200s$



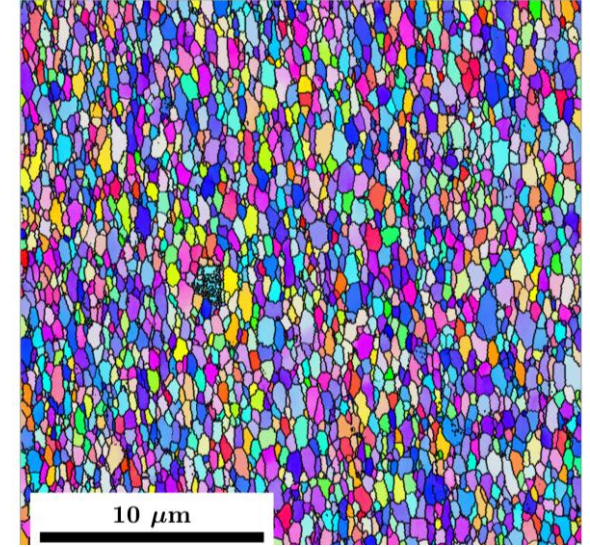
$\epsilon = 0.25, 500s$



$\epsilon = 0.5, 1000s$



$\epsilon = 0.75, 1500s$



$[\bar{1}11]$

$[\bar{1}11]$

$[\bar{1}11]$

$[\bar{1}11]$

→ Stable grain boundary sliding →

ND

ND

ND

ND

$[001]$

$[011]$

$[001]$

$[011]$

$[001]$

$[011]$

$[001]$

$[011]$



# References



- [1] Y. Saito, H. Utsunomiya, N. Tsuji, and T. Sakai, "Novel ultra-high straining process for bulk materials—development of the accumulative roll-bonding (ARB) process," *Acta Materialia*, vol. 47, no. 2, pp. 579–583, 1999.
- [2] R. M. Cleveland, A. K. Ghosh, and J. R. Bradley, "Comparison of superplastic behavior in two 5083 aluminum alloys," *Materials Science and Engineering A*, vol. 351, no. 1-2, pp. 228–236, 2003.
- [3] N. Tsuji, K. Shiotsuki, and Y. Saito, "Superplasticity of ultra-fine grained Al-Mg Alloy by ARB," *Materials Transactions*, vol. 40, no. 8, pp. 765–771, 1999.
- [4] Hsiao, I. C., and J. C. Huang. "Development of low temperature superplasticity in commercial 5083 Al-Mg alloys." *Scripta Materialia*, vol. 40, no. 6, pp. 697-703, 1999.
- [5] Hsiao, I. C., and J. C. Huang. "Deformation mechanisms during low-and high-temperature superplasticity in 5083 Al-Mg alloy." *Metallurgical and Materials Transactions A*, vol. 33, no .5, pp. 1373-1384, 2002.